the β-cells, glucose is metabolized and ATP is produced. The elevated intracellular ATP levels cause closure of K_{ATP} channels on the cell surface, which then depolarize the cell membrane leading to opening of the voltage-dependent calcium channels. The resultant influx of calcium triggers a cascade of events that result in the secretion of insulin. Overactive mutant channels as a result of activating mutations in *KCNJ11* or *ABCC8*, therefore, hyperpolarize the cell membrane, reduce calcium influx and decrease insulin secretion. Sulfonylureas bind to the SUR1 subunit of the K_{ATP} channel, and close the channel in an ATP-independent manner. It has been reported that oral sulfonylurea administration increases insulin secretion and improves metabolic control in patients with PNDM as a result of activating mutations in *KCNJ11* and *ABCC8*[7,8]. In the present study, we investigated genetic abnormalities in a patient with PNDM, and found the Pro1198Leu mutation in *ABCC8*. We examined the functional property of a mutant channel with the patch-clamp experiments, and the clinical response to oral sulfonylurea administration.

MATERIALS AND METHODS

Mutation Screening

The proband is a 12-year-old girl. She was born after 38 weeks of an uneventful pregnancy with a birthweight of 2778 g (just under the 50th percentile). At 28 weeks-of-age, she presented with severe hyperglycemia (blood glucose 915 mg/dL, glycated hemoglobin [HbA_{1c}] 12.8%) with ketoacidosis. The HbA_{1c} value was estimated as a National Glycohemoglobin Standardization Program (NGSP) equivalent value calculated by the formula HbA_{1c} = HbA_{1c} (Japan Diabetes Society [JDS]) + 0.5%, considering the relational expression of HbA_{1c} (JDS) measured by the previous Japanese standard substance and measurement methods, and HbA_{1c} (NGSP)[9]. Fasting serum C-peptide level was undetectable (<0.5 ng/mL) at first, but it was recovered to 0.9 ng/mL after 2 months of treatment with insulin. NDM is defined as diabetes with onset before 6 months-of-age in general. As her HbA_{1c} at the time of diagnosis was notably high, it could be speculated that her plasma glucose had been elevated before 6 months-of-age. Her medical record of bodyweight also suggested that failure to thrive had started from 5 months-of-age. No neurological abnormality was observed, and anti-glutamic acid decarboxylase (GAD) antibody was undetectable. Abdominal ultrasound examination at the age of 12 years showed a normally-developed pancreas. She had been treated with insulin from the onset of diabetes. The pedigree of the family is shown in Figure 1.

After obtaining written informed consent, genomic DNA was isolated from peripheral blood leukocytes. The coding regions and conserved splice sites of *KCNJ11*, *ABCC8* and *INS* were amplified from genomic DNA by polymerase chain reaction using specific primers (Supporting Information Table S1). The products were sequenced using Dye Terminator chemistry on an ABI 3100 (Applied Biosystems, Warrington, UK). The study protocol was approved by the institutional review board.

Functional Analysis of Mutant K_{ATP} Channel

The mammalian expression plasmids containing the whole coding region of the human Kir6.2 and SUR1 have been described previously[4,10]. We generated the expression plasmid of SUR1

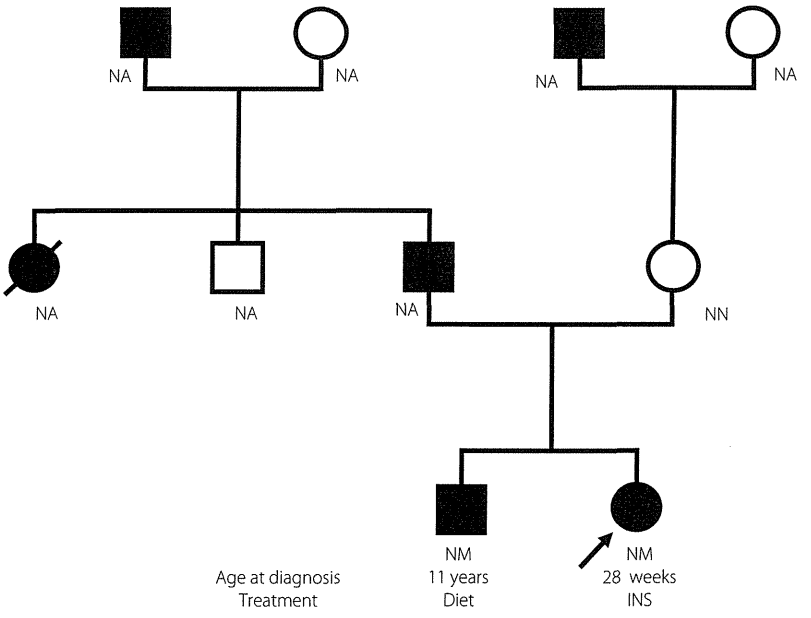

Figure 1 | Pedigree of the family. The allele status is indicated under the symbols. Directly below the genotype is the age of diagnosis of diabetes and treatment. INS, insulin; NA, not available for testing; NM, one normal and one mutated allele; NN, two normal alleles; OHA, oral hypoglycemic agent.

containing P1198L with QuickChange™ site-directed mutagenesis system (Stratagene, La Jolla, CA, USA). The presence of P1198L and the absence of other mutations were confirmed by sequencing the whole insert.

COS-1 cells were plated on 35-mm dishes containing cover slips. The cells were then transiently transfected with wild-type or mutated human SUR1 cDNA (1.5 μg per dish) plus human Kir6.2 (1.5 μg per dish) using Lipofectamine 2000 (Invitrogen, Carlsbad, CA, USA). Recordings were made 24–72 h after transfection. The ATP sensitivity of the wild-type and mutant channels were determined basically as described previously[4,10] with a patch-clamp amplifier, Axopatch 200B (Axon Instruments, Foster City, CA, USA). Sulfonylurea sensitivity was assessed as the ratio between the amplitudes of the K_{ATP} channel currents before and after tolbutamide or glibenclamide application. Data were analyzed with pCLAMP (version 9.0; Axon Instruments), XLfit (CTC Laboratory System Corporation, Tokyo, Japan) and in-house software. Unpaired Student's *t*-test was used to test for statistical significances, and the results were expressed as mean ± SE.

RESULTS

Mutation Screening

We identified a heterozygous missense mutation in *ABCC8*. The mutation results in the substitution of leucine for proline at residue 1,198 in exon 29 (c.3593 C>T, p.P1198L, GenBank NM_000352). It was not found in the databases, such as dbSNP (http://www.ncbi.nlm.nih.gov/snp/) or 1,000 genome project (http://browser.1000genomes.org/index.html), and also in 150 unrelated Japanese subjects. The mutated residue is located within the short cytosolic loop that links transmembrane domains 15 and 16. The proline (P1198) is conserved across a range of species, from mammals (human and rat) to zebrafish, and is also found at a similar position in human SUR2. The *in silico* prediction programs, SIFT (http://sift.jcvi.org/) and PolyPhen-2 (http://genetics.bwh.harvard.edu/pph2/index.shtml), both predicted that the substitution would affect protein function. No mutations associated with diabetes were found in *KCNJ11* and *INS*.

Functional Analysis of Mutant K_{ATP} Channel

We tested the sensitivity of ATP to block the wild-type and the mutant K_{ATP} channels in inside-out membrane patches (Figure 2a). The concentration of ATP required to half-maximally inhibit the channel (IC_{50}) increased ≈ sevenfold from 23.4 ± 2.5 μmol/L for wild-type channels to 164.7 ± 19.3 μmol/L for mutant channels. This result shows that the mutant channel is less ATP sensitive than the wild type.

We next tested the response to sulfonylureas for the wild-type and the mutant K_{ATP} channels in inside-out membrane patches in nucleotide-free condition (Figure 2b). A total of 100 μmol/L tolbutamide inhibited the current by 65.6 ± 4.8% for the mutant channel, whereas 19.3 ± 5.2% for the wild type. In contrast, 30 nmol/L glibenclamide inhibited the current by 44.5 ± 6.5% for the mutant channel, whereas 10.8 ± 2.7% for the wild type. The residual current in the presence of

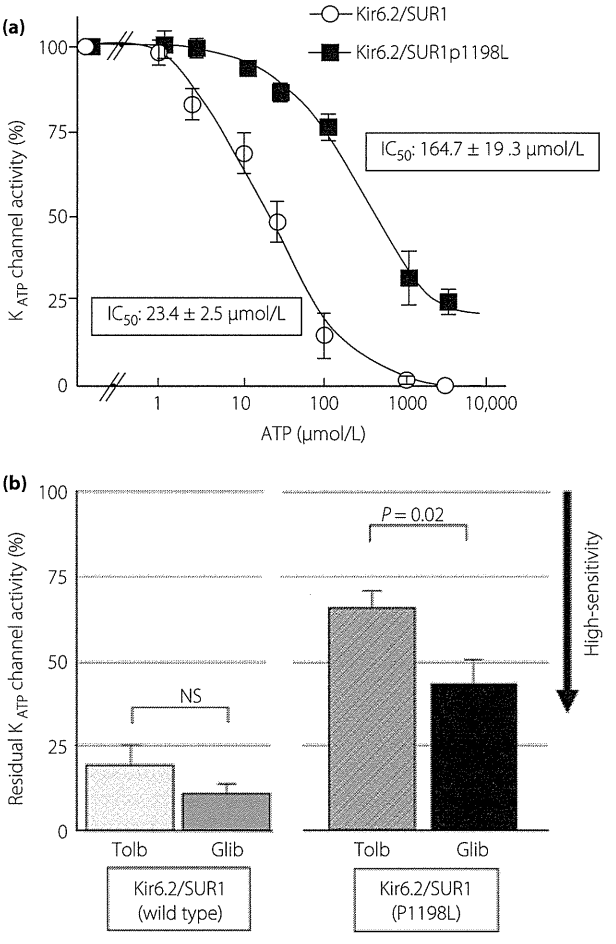

Figure 2 | (a) Adenosine triphosphate (ATP) sensitivity of wild-type and mutant ATP-sensitive potassium (K_{ATP}) channels. The dose-dependent inhibitory effects of ATP on the activities of the wild-type (Kir6.2/SUR1) and mutant (Kir6.2/SUR1P1198L) K_{ATP} channels are shown. Five experiments were carried out for each type of channel. The channel conductance of the mutant channel in a ATP-free condition was similar to that of the wild-type channel (73.1 ± 0.57 vs 72.9 ± 0.52 pico-siemens (pS), P = 0.765). (b) Sulfonylurea sensitivity of the wild-type (Kir6.2/SUR1) or the mutant (Kir6.2/SUR1P1198L) K_{ATP} channels. Residual K_{ATP} channel activities were determined by the ratio between the amplitudes of K_{ATP} channel currents before and after 100 μmol/L tolbutamide (Tolb) or 30 nmol/L glibenclamide (Glib) applications. Data are mean ± standard error from seven independent experiments. IC_{50}, the concentration of adenosine triphosphate at which the inhibition is half of the maximal.

glibenclamide for the mutant channel was significantly smaller than that of tolbutamide (P = 0.02). These results show that the sensitivity to sulfonylureas is reduced in the mutant channel and glibenclamide is more effective than tolbutamide.

Clinical Effectiveness of Oral Sulfonylurea Therapy

After identification of an *ABCC8* gene mutation, the patient's treatment was switched from insulin injection (40 units a day)

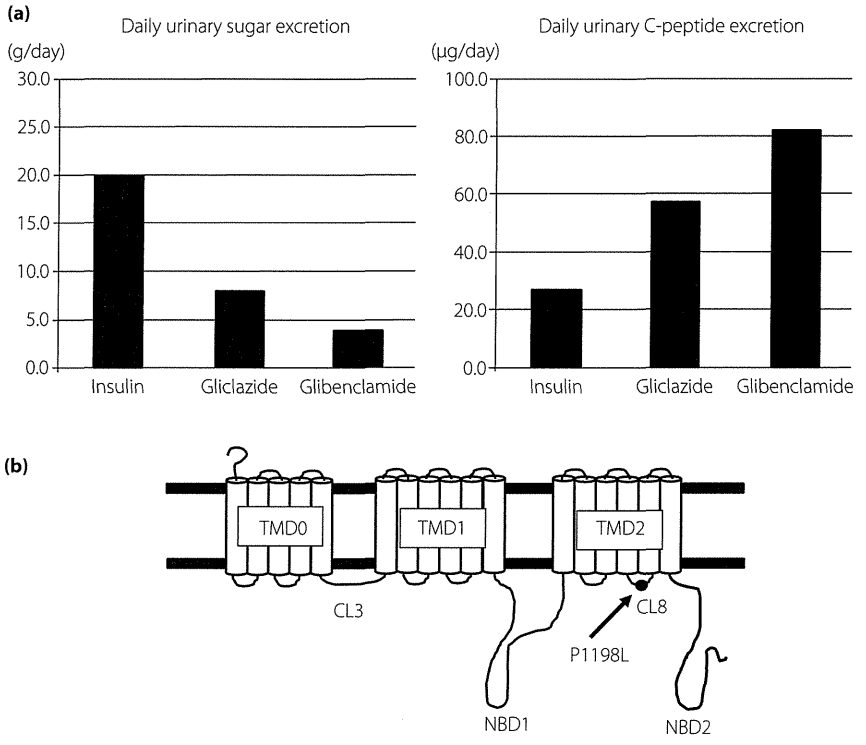

Figure 3 | (a) Daily urinary sugar excretion and daily urinary C-peptide excretion at insulin injection, high-dose gliclazide (a daily dose of 160 mg) or low-dose glibenclamide (a daily dose of 0.625 mg, which is 0.017 mg/kg/day) administration in the patient. (b) Schematic representation of the sulfonylurea receptor and the location of P1198L mutation (arrowed) identified in the patient. CL, cytosolic loop; NBD, nucleotide-binding domain; TMD, transmembrane domain.

to oral sulfonylureas under intensive monitoring in the hospital. Daily urinary C-peptide excretion, which was 27.8 μg/day before initiating sulfonylureas, increased to 58.1 μg/day at high-dose gliclazide (a daily dose of 160 mg) alone. Furthermore, daily urinary C-peptide excretion was further increased to 83 μg/day at low-dose glibenclamide (a daily dose of 0.625 mg, which is 0.017 mg/kg/day; Figure 3a). Simultaneously, daily urinary sugar excretion was decreased in inverse proportion to urinary C-peptide excretion (20.0, 8.0 and 4.0 g/day, respectively). Thus, oral glibenclamide treatment was selected for the patient's therapy and insulin injection was completely discontinued. Her blood glucose level was finally controlled with 0.17 mg/kg/day of glibenclamide.

DISCUSSION

In the present study, we identified the Pro1198Leu mutation in a patient with PNDM. The mutation was not found in the databases, such as dbSNP or 1,000 genome project, and also in 150 unrelated Japanese subjects. Furthermore, two *in silico* prediction programs, SIFT and PolyPhen-2, predicted that the mutation would affect protein function. We further confirmed that the mutant channel was less ATP sensitive than the wild type with a patch-clamp experiment. The degree of ATP insensitivity was comparable with that in a previous report for PNDM as a result of activating mutations in *ABCC8*[11]. These findings suggest that the P1198L mutation is strongly associated with the development of PNDM in the patient. Furthermore, it has only recently been reported from Turkey that the same mutation was identified in a girl with NDM[12]. In that report, the patient presented with severe hyperglycemia with ketoacidosis at 1 month-of-age and was initially treated with insulin. After genetic diagnosis, her treatment was successfully converted from insulin to glibenclamide (0.2 mg/kg/day). In addition, no neurological abnormality and no family history of diabetes were observed in the patient. These clinical characteristics were similar to the present case, except there was no family history of diabetes. In contrast, *in vitro* functional analysis of the mutation was not carried out in the report.

The mutated residue P1198 is located within the eighth cytosolic loop (CL8) that links transmembrane domains 15 and 16 in the SUR1 (Figure 3b). This loop has been reported to be a binding site of tolbutamide[13], and our functional analysis also showed that the sensitivity to tolbutamide was reduced in the mutant channel. Based on the drug structure, gliclazide is also thought to bind to the CL8. In contrast, in addition to the CL8, glibenclamide is able to bind to another site in the SUR1, which is located within the third cytosolic loop (CL3)[14]. This could explain the reason why glibenclamide was more effective both in patch-clamp experiments and in the patient.

In the family of the patient, her elder brother carried the P1198L mutation in the heterozygous state, whereas her mother did not (Figure 1). This suggests a possibility that her father might have the same mutation. The elder brother was diagnosed with diabetes at 11 years-of-age on medical examination at his school, but his diabetes was very mild and has been treated with diet alone. Furthermore, the proband's father, paternal aunt and paternal grandfather have diabetes. However, there is little information on these members, because her parents have divorced and members of her father's family did not agree to cooperate in the present study. The phenotypic variability of diabetes within families has been reported in some families with *ABCC8* gene mutations[8,15]. The precise reason for the variability is currently unknown. It might be explained by the influence of unknown other genetic and/or epigenetic factors.

Many patients with PNDM caused by *ABCC8* or *KCNJ11* gene mutations have been successfully treated with sulfonylureas[7,8]. In the present study, the treatment of our patient was also able to be switched from insulin injection to oral sulfonylurea therapy. In contrast, response to sulfonylureas has not been seen in PNDM caused by other gene mutations, such as *INS*[1]. This suggests that genetic diagnosis can provide clinical benefits to the patients with PNDM. It has been reported that genetic testing for *KCNJ11* and *ABCC8* in all children diagnosed before 6 months-of-age results not only in improved quality of life, but also in cost savings[16]. However, a large number of patients with PNDM have still been misdiagnosed as a very early onset form of type 1 diabetes and treated with insulin. The genetic diagnosis of PNDM will take on a growing importance in clinical practice.

ACKNOWLEDGEMENTS

The present study was supported by Scientific Research Grants from the Ministry of Education, Culture, Sports, Science and Technology of Japan, and from the Ministry of Health, Labor and Welfare of Japan. The authors declare no financial support or relationships that may pose a conflict of interest.

REFERENCES

1. Naylor RN, Greeley SA, Bell GI, *et al.* Genetics and pathophysiology of nenonatal diabetes mellitus. *J Diabetes Invest* 2011; 2: 158–169.
2. Suzuki S, Makita Y, Mukai T, *et al.* Molecular basis of neonatal diabetes in Japanese patients. *J Clin Endocrinol Metab* 2007; 92: 3979–3985.
3. Temple IK, Gardner RJ, Mackay DJ, *et al.* Transient neonatal diabetes: widening the understanding of the etiopathogenesis of diabetes. *Diabetes* 2000; 49: 1359–1366.
4. Inagaki N, Gonoi T, Clement JPT, *et al.* Reconstitution of IKATP: an inward rectifier subunit plus the sulfonylurea receptor. *Science* 1995; 270: 1166–1170.
5. Flanagan SE, Patch AM, Mackay DJ, *et al.* Mutations in ATP-sensitive K+ channel genes cause transient neonatal diabetes and permanent diabetes in childhood or adulthood. *Diabetes* 2007; 56: 1930–1937.
6. Edghill EL, Flanagan SE, Patch AM, *et al.* Insulin mutation screening in 1,044 patients with diabetes: mutations in the INS gene are a common cause of neonatal diabetes but a rare cause of diabetes diagnosed in childhood or adulthood. *Diabetes* 2008; 57: 1034–1042.
7. Pearson ER, Flechtner I, Njolstad PR, *et al.* Switching from insulin to oral sulfonylureas in patients with diabetes due to Kir6.2 mutations. *N Engl J Med* 2006; 355: 467–477.
8. Babenko AP, Polak M, Cave H, *et al.* Activating mutations in the *ABCC8* gene in neonatal diabetes mellitus. *N Engl J Med* 2006; 355: 456–466.
9. Kashiwagi A, Kasuga M, Araki E, *et al.* International clinical harmonization of glycated hemoglobin in Japan: from Japan Diabetes Society to National Glycohemoglobin Standardization program values. *J Diabetes Invest* 2012; 3: 39–40.
10. Beguin P, Nagashima K, Nishimura M, *et al.* PKA-mediated phosphorylation of the human K(ATP) channel: separate roles of Kir6.2 and SUR1 subunit phosphorylation. *EMBO J* 1999; 18: 4722–4732.
11. Ellard S, Flanagan SE, Girard CA, *et al.* Permanent neonatal diabetes caused by dominant, recessive, or compound heterozygous SUR1 mutations with opposite functional effects. *Am J Hum Genet* 2007; 81: 375–382.
12. Oztekin O, Durmaz E, Kalay S, *et al.* Successful sulfonylurea treatment of a neonate with neonatal diabetes mellitus due to a novel missense mutation, p.P1199L, in the *ABCC8* gene. *J Perinatol* 2012; 32: 645–647.
13. Ashfield R, Gribble FM, Ashcroft SJ, *et al.* Identification of the high-affinity tolbutamide site on the SUR1 subunit of the K(ATP) channel. *Diabetes* 1999; 48: 1341–1347.
14. Mikhailov MV, Mikhailova EA, Ashcroft SJ. Molecular structure of the glibenclamide binding site of the beta-cell K(ATP) channel. *FEBS Lett* 2001; 499: 154–160.
15. Patch AM, Flanagan SE, Boustred C, *et al.* Mutations in the *ABCC8* gene encoding the SUR1 subunit of the KATP channel cause transient neonatal diabetes, permanent neonatal diabetes or permanent diabetes diagnosed outside the neonatal period. *Diabetes Obes Metab* 2007; 9(Suppl 2): 28–39.
16. Greeley SA, John PM, Winn AN, *et al.* The cost-effectiveness of personalized genetic medicine: the case of genetic testing in neonatal diabetes. *Diabetes Care* 2011; 34: 622–627.

SUPPORTING INFORMATION

Additional Supporting Information may be found in the online version of this article:

Table S1 | Primer sequences for amplification of *ABCC8* gene

Clinical Nutrition 32 (2013) 777–782

Contents lists available at SciVerse ScienceDirect

Clinical Nutrition

journal homepage: http://www.elsevier.com/locate/clnu

Original article

A new equation to estimate basal energy expenditure of patients with diabetes☆

Kaori Ikeda [a], Shimpei Fujimoto [a,b], Masashi Goto [c], Chizumi Yamada [a], Akihiro Hamasaki [a], Megumi Ida [d], Kazuaki Nagashima [a], Kenichiro Shide [d], Takashi Kawamura [c], Nobuya Inagaki [a,*]

[a] Department of Diabetes and Clinical Nutrition, Graduate School of Medicine, Kyoto University, 54 Shogoin Kawahara-cho, Sakyo-ku, Kyoto 606-8507, Japan
[b] Department of Endocrinology, Metabolism and Nephrology, Kochi Medical School, Japan
[c] Kyoto University Health Service, Japan
[d] Department of Metabolism and Clinical Nutrition, Kyoto University Hospital, Japan

ARTICLE INFO

Article history:
Received 17 February 2012
Accepted 22 November 2012

Keywords:
Basal metabolic rate
Resting metabolic rate
Indirect calorimetry
Prediction equation
Diabetes
Medical nutrition therapy

SUMMARY

Background & aims: Predictive equations for basal energy expenditure (BEE) derived from Caucasians tend to overestimate BEE in non-Caucasians. The aim of this study was to develop a more suitable method to estimate BEE in Japanese patients with diabetes using indices readily measured in clinical practice.

Methods: BEE was measured by indirect calorimetry under a strict basal condition in 68 Japanese patients with type 1 or type 2 diabetes. The best fitting equation was investigated by multiple regression analysis using of age, sex, and anthropometric indices. The resultant new equation was tested in a separate group of 60 Japanese patients with type 1 or type 2 diabetes, and the accuracy compared with existing equations.

Results: The best-fit equation was BEE [kcal/day] = 10 × (body weight)[kg] − 3 × (age)[y] + 125 (if male) + 750. Adjusted coefficient of determination was 81.0%. Root mean squared errors and accurate prediction in the validation set were 103 kcal/day and 78% for the new equation; 184 and 50 for Harris-Benedict; 209 and 38 for Oxford; 205 and 42 for Liu; and 140 and 63 for Ganpule.

Conclusions: This new equation is simpler and estimates BEE more accurately in Japanese patients with diabetes than the presently used equations do.

1. Introduction

Diet is the most fundamental and initial treatment for all patients with diabetes, and poor dietary management alone predicts poor subsequent glycemic control.[1] Estimation of daily energy expenditure for each patient is necessary for effective individualized diabetic meal planning. Resting energy expenditure (REE) or basal energy expenditure (BEE) is defined as the energy expended to maintain minimal metabolic activities, and is the main component of total daily energy expenditure. To estimate daily energy expenditure, REE or BEE is multiplied by a number specific to the various daily activities.

In healthy subjects, 65–90% of inter-individual variation in REE is explained by fat-free mass (FFM).[2] In patients with diabetes, FFM is also the main factor in REE and BEE,[3-5] and there is no difference in FFM-adjusted REE between mildly hyperglycemic patients and controls.[6] In clinical practice, BEE or FFM are not usually available. Equations factoring body weight, height, age and sex are widely used for clinical estimation of the daily energy requirement of patients with diabetes.[7] However, there has been little investigation of the comparative validity of these equations.

The existing predictive equations derived from Caucasians are unevenly applied to non-Caucasians, tending to overestimate energy expenditure.[8–11] This accords with the recent finding from the basal metabolic rate database that BEE is higher in Caucasians than in non-Caucasians.[12] However, REE is similar in Asians and Caucasians after adjustment for FFM, and BEE in Indians and

☆ A part of this study was presented in abstract form at the annual meeting of American Diabetes Association, New Orleans, Louisiana, 5–9 June 2009.

* Corresponding author. Tel.: +81 75 751 3562; fax: +81 75 771 6601.
E-mail addresses: kaikeda@metab.kuhp.kyoto-u.ac.jp (K. Ikeda), fujimoto@kochi-u.ac.jp (S. Fujimoto), goto@msa.biglobe.ne.jp (M. Goto), chizumi-y@nifty.com (C. Yamada), hamasaki@metab.kuhp.kyoto-u.ac.jp (A. Hamasaki), idamegu@kuhp.kyoto-u.ac.jp (M. Ida), nagasima@metab.kuhp.kyoto-u.ac.jp (K. Nagashima), shide@kuhp.kyoto-u.ac.jp (K. Shide), kawax@kuhp.kyoto-u.ac.jp (T. Kawamura), inagaki@metab.kuhp.kyoto-u.ac.jp (N. Inagaki).

0261-5614/$ – see front matter © 2012 Elsevier Ltd and European Society for Clinical Nutrition and Metabolism. All rights reserved.
http://dx.doi.org/10.1016/j.clnu.2012.11.017

Australians is similar after adjustment for FFM and fat mass.[13,14] To date, there are few equations to estimate energy expenditure specifically in Asian populations.[10,15]

Differences in the measurement technique of REE can cause biases.[12] In most studies evaluating energy expenditure, REE has been used rather than BEE. However, REE is defined less rigorously than BEE and is influenced by physical and psychological stress and ambient and body temperature.[16–18] Since BEE is measured early in the morning before the subject begins any physical activity and at least 10 h after ingestion of any food, drink, or nicotine, it remains remarkably constant on a daily basis.[16,18]

In the present study, by measuring BEE under strict conditions, we developed a new equation for estimation of BEE in Japanese patients with diabetes for use in a clinical setting.

2. Patients, materials and methods

2.1. Patients

Japanese patients with type 1 or type 2 diabetes admitted to the Department of Diabetes and Clinical Nutrition, Kyoto University Hospital, Kyoto, Japan for diabetes self-management education during the period of December 2007 through September 2009 were recruited for derivation study. Written, informed consent was obtained from all participants. During hospital stay, the participants had a prescribed diet with or without medications including oral hypoglycemic agents and insulin according to the treatment guide for diabetes of the Japan Diabetes Society.[19] Their physical activity was not restricted, but they did not engage in vigorous exercise. Participants were screened by medical history, physical examination, and laboratory testing to assure the absence of hepatic, pulmonary, thyroid, cardiac and renal dysfunction, macroalbuminuria, inflammatory diseases, and malignant tumors. Those who took steroids or beta blockers or had physical disabilities were excluded. The study protocol was approved by Kyoto University Graduate School and Faculty of Medicine, Ethics Committee.

2.2. Indirect calorimetry

Basal energy expenditure (BEE) was measured in the morning under glycemic control with prescribed diet (29.1 ± 2.5 kcal/kg of standard body weight per day consisting of 52% carbohydrate, 20% protein, and 28% fat in energy component) and with medications when needed. Standard body weight (kg) was calculated by multiplying 22 (kg/m^2) by square of height (m). Whole-body oxygen consumption (VO_2) and carbon dioxide production (VCO_2) was measured for more than 10 min with indirect calorimetry (AE300S, Minato Medical Science, Osaka, Japan) by one investigator (KI) at the bedside of each patient under the strict condition described previously.[5,16,17] Briefly, an afebrile patient in a post-absorptive state after an overnight fast (14 h) with <180 mg/dL capillary plasma glucose remained in a supine position after waking on the bed in the ward without smoking or taking caffeine, and the measurements were performed at room temperature between 22 °C and 27 °C. After discarding the initial 5 min of recording, we took 5-min of data, in accord with the steady state definition,[17] during which the coefficient of variation for VO_2 per minute and VCO_2 per minute was achieved ≤10%, and applied them to the Weir formula with 24-h urinary urea nitrogen.[20]

2.3. Anthropometry and body composition

Height was measured on the day of admission. Body weight, skinfold thickness, and waist circumference were measured immediately after the measurement of BEE by one investigator (KI). Triceps-skinfold thickness (TSF) and mid-upper arm circumference (MAC) were measured in the non-dominant arm with the elbow bent at 90°. The physical markers were measured at least twice, and their respective mean values expressed according to Japanese standard method.[21] Arm muscle circumference (AMC) and arm muscle area (AMA) were calculated; AMC [cm] = MAC [cm] − π × TSF [mm]/10, AMA [cm^2] = (AMC [cm])^2 / 4π. Waist circumference was measured at the mid-point between the lowest rib and the iliac crest in a standing position at the end of gentle expiration keeping the measuring tape horizontal and just fitted to the skin. Hip circumference was measured at the widest part of the hip while standing. FFM and fat mass were measured by dual energy X-ray absorptiometry scanner (Discovery, Hologic, Bedford, MA, USA) within 3 days before and after measurement of BEE.

2.4. Other measurements

Glycated hemoglobin was measured by use of HPLC (ADAMS™ A1C HA8180, Arcray, Kyoto, Japan) and expressed as a National Glycohemoglobin Standardization Program (NGSP) equivalent value [%] calculated by the formula HbA1c [%] = HbA1c [Japan Diabetes Society (JDS)] [%] + 0.4 [%], which considers the relational expression of HbA1c (JDS) measured by the previous Japanese standard substance and measurement methods and HbA1c (NGSP).[22] Capillary glucose before each meal was measured by glucose meter (One Touch Ultra™, Johnson & Johnson, New Brunswick, NJ, USA) and expressed as capillary plasma glucose (PG). As a parameter of glycemic control, mean preprandial PG for three consecutive days before the measurement of BEE and fasting PG (FPG) just before the measurement of BEE are shown.

2.5. Testing the new equation

A separate data set of Japanese patients with type 1 or type 2 diabetes admitted to the same department for the same purpose during the period of June 2005 through December 2007 was drawn from the medical records for validation study. Inclusion/exclusion criteria and dietary condition during hospital stay were similar to that of the derivation sample.

Whole-body VO_2 and VCO_2 was measured after an overnight fast (14–16 h) for more than 15 min with the same calorimetry by one investigator (MI) on the same condition. Each patient was conveyed from their ward to the examination room by a healthcare staff member in a wheel chair and they rested in bed in a supine position for 30 min before the measurement of BEE. BEE was calculated from VO_2 and VCO_2 by use of Elwyn formula (BEE [kcal/day] = 3.581 × VO_2 [L/day] + 1.448 × VCO_2 [L/day] − 32.4).[16] Body weight was measured on the day of calorimetry.

The protocol of this validation study was also approved by Kyoto University Graduate School and Faculty of Medicine, Ethics Committee.

2.6. Statistical analysis

Numerical data are summarized as means ± SDs. Categorical data were treated as dummy variables.

We first explored good estimators for FFM and fat mass in anthropometric indices, such as body weight, height, TSF, AMA, waist circumference and hip circumference, because FFM and fat mass are known as two major estimators of BEE. Correlations between these variables were evaluated by Pearson's correlation analysis. Multiple linear regression analysis was then performed to evaluate the contribution of anthropometric indices, age, and sex to FFM and fat mass. Next, a best-fit equation to estimate BEE from anthropometric indices, age, and sex was explored by multiple

linear regression analysis with consideration of estimators of FFM and fat mass.

For testing the validity of our new equation and comparing it with existing prediction equations, we calculated measures of accuracy. The mean percentage difference between BEE estimated and measured (bias) was considered systematic error. The root mean squared error (RMSE) was considered to reflect each individual's error range unrelated to whether it was over or under estimation. The proportion of patients with BEE estimated within ±10% of BEE measured was considered another measure of accuracy.[23]

Data were analyzed by use of Stata 11.0 (Stata Corporation, College Station, TX, USA). Statistical significance was set at $P < 0.05$ (2-tailed).

3. Results

Data were obtained and analyzed in 68 patients, of which 7 had type 1 diabetes and 61 had type 2 diabetes. Mean glycated hemoglobin (HbA1c) on admission was as high as 10.5%, but mean fasting plasma glucose just before the measurement of BEE (FPG) was as low as 113.7 mg/dL due to the treatments during hospital stay (Table 1). Additional characteristics of patients in the derivation set and the results of measurement are shown in Table 1.

Body weight had the highest correlation with FFM ($r = 0.90$), followed by arm muscle area (AMA), height and hip circumference ($r = 0.84$, 0.75 and 0.73, respectively) (Table 2). Waist circumference had the highest correlation with fat mass ($r = 0.91$), followed by hip circumference, triceps-skinfold thickness (TSF) and body weight ($r = 0.79$, 0.78 and 0.75, respectively).

Table 1
Characteristics of patients (derivation set).

	All	Male	Female
No. of patients	68	39	29
Type of diabetes (type1/type2) (n)	7/61	4/35	3/26
Age (years)	59.8 ± 11.2 (range 19–78)	58.3 ± 10.3	61.8 ± 12.2
Height (cm)	161.3 ± 9.5	167.6 ± 6.0	152.9 ± 6.3
Body weight (kg)	62.8 ± 14.7 (range 34.6–113.6)	67.3 ± 16.0	56.7 ± 10.2
BMI (kg/m^2)	24.0 ± 4.7	23.9 ± 5.3	24.2 ± 3.8
FFM (kg)	47.7 ± 10.6	53.4 ± 9.4	39.9 ± 6.5
Fat mass (kg)	16.0 ± 7.0	14.8 ± 8.0	17.8 ± 4.9
TSF (mm)	15.9 ± 7.8	13.1 ± 6.5	19.8 ± 7.8
AMA (cm^2)	44.6 ± 10.2	48.9 ± 9.7	38.8 ± 7.9
Waist (cm)	86.5 ± 12.4	86.2 ± 14.0	86.9 ± 10.3
Hip (cm)	91.3 ± 7.8	92.4 ± 8.5	89.8 ± 6.7
BEE (kcal/day)	1290 ± 217	1395 ± 210	1149 ± 130
FPG (mg/dL)	113.7 ± 25.8	113.3 ± 25.5	114.3 ± 26.6
PPPG (mg/dL)	143.5 ± 35.9	146.5 ± 39.7	139.3 ± 30.3
HbA1c (%)	10.5 ± 2.5	10.3 ± 2.4	10.8 ± 2.7
Duration of diabetes (years)	9.3 ± 7.8	10.9 ± 8.9	7.1 ± 5.5
Treatment			
Diet (kcal/SBW/day)	29.1 ± 2.5	28.9 ± 2.1	29.3 ± 3.0
Medications			
Ins only (n)	34	21	13
Ins + Met (n)	10	4	6
Ins + SU (n)	3	2	1
Ins + SU + Met (n)	1	0	1
SU (n)	8	5	3
SU + Met (n)	5	2	3
Met only (n)	4	3	1
None (n)	3	2	1

Data are means ± SD. BMI, body mass index; FFM, fat-free mass; TSF, triceps-skinfold thickness; AMA, arm muscle area; Waist, waist circumference; Hip, hip circumference; BEE, basal energy expenditure; FPG, fasting plasma glucose just before the measurement of BEE; PPPG, mean preprandial plasma glucose for three consecutive days before the measurement of BEE; HbA1c, glycated hemoglobin; SBW, standard body weight; Ins, insulin; SU, sulfonylurea; Met, metformin.

Table 2
Correlations between FFM, fat mass and anthropometric indices.

	FFM	FM	Ht	Wt	TSF	AMA	Waist	Hip
FFM	1.00	–	–	–	–	–	–	–
FM	0.38†	1.00		–	–	–	–	–
Ht	0.75‡	−0.12	1.00	–	–	–	–	–
Wt	0.90‡	0.75‡	0.49‡	1.00	–	–	–	–
TSF	0.13	0.78‡	−0.30*	0.46‡	1.00	–	–	–
AMA	0.84‡	0.48†	0.50‡	0.83‡	0.07	1.00	–	–
Waist	0.56‡	0.91‡	0.02	0.83‡	0.70‡	0.60‡	1.00	–
Hip	0.73‡	0.79‡	0.28*	0.90‡	0.50‡	0.73‡	0.83‡	1.00

Pearson's correlation coefficients ($n = 68$): *$p < 0.05$; †$p < 0.01$; ‡$p < 0.001$. FFM, fat-free mass; Ht, height; Wt, weight; TSF, triceps-skinfold thickness; AMA, arm muscle area; Waist, waist circumference; Hip, hip circumference.

In regression analysis for FFM, we selected body weight, AMA, height and hip circumference as potent estimators together with other plausible estimators, age and sex. As both AMA and hip circumference were strongly correlated with body weight and AMA was also strongly correlated with hip circumference, to analyze these three variables separately, we used three sets of independent variables, (body weight, height, age and sex), (AMA, height, age and sex), and (hip circumference, height, age and sex). The regressions revealed that all four variables were significant estimators for FFM in the first analysis (model 1 in Table 3), that AMA and height were significant in the second analysis (model 2) and that hip circumference, height and sex were significant in the third analysis (model 3). The first four variables accounted for 95% of variation in FFM, the second two variables 84%, and the third three variables 87%. For fat mass, we selected another three sets of independent variables, (waist circumference, age and sex), (hip circumference, TSF, age and sex) and (body weight, TSF, age and sex) because waist circumference had a strong correlation with hip circumference, TSF and body weight, and hip circumference also had a strong correlation with body weight. In the first analysis, only waist circumference and sex were significant estimators for fat mass, accounting for 86% of fat mass (model 4). In the second analysis, hip circumference, TSF and age were significant, accounting for 84% of fat mass (model 5). In the third analysis, body weight, TSF, age and sex were significant, accounting for 87% of fat mass (model 6).

We performed regression analysis to determine BEE with the most influential estimators (FFM and fat mass) and plausible additional estimators (age and sex), which together explained 81% of the variation (model 7 in Table 3). We then performed backward stepwise estimation, using three sets of variables, (significant variables in model 1 and 6; body weight, height, TSF, age and sex), (significant variables in model 2 and 4 plus age; AMA, height, waist, sex and age), and (significant variables in model 3 and 5; hip circumference, height, TSF, age and sex). The best fitting regression for BEE consisted of body weight, age and sex in the first analysis (model 8), height, waist, age and sex in the second analysis (model 9), and hip circumference, height, TSF and sex in the third analysis (model 10). The adjusted coefficient of determination in model 8 was 81%, which was larger than the 73% in model 9 and the 77% in model 10. The detailed results of model 8 are shown in Table 4.

We then simplified the resultant equation of model 8 to make it easy to use in clinical practice.

$$\mathrm{BEE} = 10 \times \text{body weight} - 3 \times \text{age} + 125(\text{if male}) + 750.$$

[BEE (kcal/day), body weight (kg), age (year)]

The bias of this equation in the derivation set was − 1.2 ± 6.4%; RMSE was 94 kcal/day; accurate estimation was 91%.

Table 3
Results of multiple regressions for FFM, FM and BEE.

	Adj. R^2		Model
FFM = −26.9 + 0.5 × Wt + 0.3 × Ht − 0.1 × Age + 3.9 × Sex[a]	0.95		1
FFM = −60.8 + 0.6 × AMA + 0.5 × Ht[b]	0.84		2
FFM = −102.8 + 0.8 × Hip + 0.5 × Ht + 4.5 × Sex[c]	0.87		3
FM = −26.3 + 0.5 × Waist − 2.6 × Sex[c]	0.86		4
FM = −45.4 + 0.5 × Hip + 0.4 × TSF + 0.1 × Age[d]	0.84		5
FM = −14.3 + 0.4 × Wt + 0.2 × TSF + 0.1 × Age − 5.1 × Sex	0.87		6
BEE = 691.6 + 11.6 × FFM + 8.9 × FM − 2.6 × Age + 106.7 × Sex	0.81		7
BEE = 748.4 + 10.4 × Wt − 3.0 × Age + 125.4 × Sex[e]	0.81	Model (1 + 6)	8
BEE = −332.3 + 6.1 × Ht + 9.5 × Waist − 4.6 × Age + 147.1 × Sex[f]	0.73	Model (2 + 4)	9
BEE = −1139.3 + 13.8 × Hip + 6.1 × Ht + 5.6 × TSF + 157.9 × Sex[c]	0.77	Model (3 + 5)	10

FFM, fat-free mass (kg); FM, fat mass (kg); BEE, basal energy expenditure (kcal/day); Wt, body weight (kg); Ht, height (cm); AMA, arm muscle area (cm^2); Hip, hip circumference (cm); Waist, waist circumference (cm); TSF, triceps-skinfold thickness (mm); Adj. R^2, adjusted coefficient of determination.
[a] Male = 1, female = 0.
[b] Age and sex were not significant determinants when added to this model.
[c] Age was not a significant determinant when added to this model.
[d] Sex was not a significant determinant when added to this model.
[e] Height and TSF were not significant determinants when added to this model.
[f] AMA was not a significant determinant when added to this model.

We then tested this new equation in a separate validation data set comparing it with existing equations (Table 5). Characteristics of patients in the validation set are shown in Table 6. The ratio of patients with type 1 and 2 diabetes was almost the same as in the derivation set. Mean age was similar to that in the derivation set, but there were more obese people in the validation set. FPG and PPPG, which represent the glycemic levels around the time of measurement of BEE, were higher, but HbA1c on admission was lower than that in the derivation set. Mean duration of diabetes was similar to that in the derivation set. Prescribed diet was almost the same as in the derivation set, but treatment with insulin was more common in the derivation set. The bias of the new equation was 4.8 ± 7.7%, RMSE was 103 kcal/day, and the percent of patients estimated within ±10% of measured value was 78%. The new equation had better validity than Harris and Benedict equation, Oxford equation, or the Liu equation and Ganpule equation (Table 7).

4. Discussion

We report a new equation to estimate BEE in Japanese patients with diabetes with higher accuracy compared to existing equations. As in other BEE estimation equations, the main estimator was FFM and additional estimators were fat mass, age and sex.[2–4,24] Stepwise estimation analysis of the estimators of FFM and fat mass in the present study revealed that no other indices improved fitting of the equation for BEE except body weight, age and sex. Although anthropometric indices are good estimators for body composition and they improve predictability of certain equations for BEE,[25,26] they were not as effective as body weight in the present study.

Table 4
Detailed result of model 8.

Dependent variable BEE[a]	Coef.[b]	95% CI[c]		Std. coef.[d]	$P > t$	Adj. R^2[e]
Independent variables						
Intercept	748.4	562.6	934.1		<0.001	0.810
Wt (kg)	10.4	8.6	12.1	0.70	<0.001	
Age (year)	−3.0	−5.2	−0.9	−0.16	0.007	
Sex (male = 1, female = 0)	125.4	75.6	175.1	0.29	<0.001	

[a] BEE, basal energy expenditure (kcal/day).
[b] Coef., partial regression coefficient.
[c] CI, confidence interval.
[d] Std. coef., standardized coefficient.
[e] Adj. R^2, adjusted coefficient of determination.

This accords with the finding that the standard error of the estimate of REE prediction by weight, height, sex and age was well within the range of the standard error of estimates from other FFM-derived prediction equation.[27] Since ethnic difference in BEE is derived from differences in body composition,[13] an ethnicity-specific constant term could more precisely estimates BEE,[4,12] but an ethnicity-specific coefficient of anthropometry is also valid.

We compared our new equation with existing equations such as Harris and Benedict, Oxford, Liu, and Ganpule because the Harris and Benedict equation is widely known in clinical practice in Japan, the Oxford equation was recently developed from a large number of subjects including many ethnicities, and the Liu equation and Ganpule equations were derived from Chinese and Japanese subjects, respectively.[7,10,12,15] The validation analysis revealed better validity of the new equation in Japanese patients with diabetes than any of the other equations.

BEE was measured under strictly controlled conditions in the present study. In addition, we confirmed the FPG of the patients to be < 180 mg/dL just before the measurement of BEE, since BEE is unaffected by the glucose level when its value is < 180 mg/dL.[5,6] As the mean FPG of patients in the derivation set was improved to 114 mg/dl just before the measurement of BEE due to the prescribed diet and medications during hospital stay, in contrast to the poor mean FPG level as high as 170 mg/dl just after admission, clinical application of this equation to patients with stable glycemic control is recommended.

Table 5
Equations to estimate BEE.[a]

	Formula	Reference
New equation	10 W − 3 A + 125 (if male) + 750[b,c]	
Harris and Benedict (1919)	Male: 13.75 W + 5.00 H − 6.76 A + 66.47[d] Female: 9.56W + 1.85 H − 4.68 A + 655.10	7
Oxford (2005)	Male: 18–30 years; 16.0 W + 545 30–60 years; 14.2 W + 593 60 + years; 13.5 W + 514 Female: 18–30 years; 13.1 W + 558 30–60 years; 9.74 W + 694 60 + years; 10.1 W + 569	12
Liu (1995)	13.88 W + 4.16 H−3.43 A − 112.40 (if female) + 54.34	10
Ganpule (2007)	(48.1 W + 23.4 H−13.8 A−547.3(if female) − 423.5)/4.186	15

[a] BEE, basal energy expenditure (kcal/day).
[b] W, weight (kg).
[c] A, age (year).
[d] H, height (cm).

Table 6
Characteristics of patients (validation set).

	All	Male	Female
No. of patients	60	36	24
Type of diabetes (type1/type2) (n)	6/54	3/33	3/21
Age (years)	58.9 ± 13.3 (range 21–82)	55.8 ± 13.5	63.6 ± 11.8
Body weight (kg)	66.9 ± 18.2 (range 41.1–138.0)	70.0 ± 19.2	62.2 ± 15.8
BMI (kg/m^2)	25.7 ± 6.7	24.6 ± 6.2	27.5 ± 7.2
BEE (kcal/day)	1260 ± 219	1342 ± 225	1137 ± 141
FPG (mg/dL)	132.1 ± 20.8	130.8 ± 20.5	133.9 ± 21.6
PPPG (mg/dL)	157.6 ± 32.3	156.7 ± 34.8	159.0 ± 28.9
HbA1c (%)	9.3 ± 1.5	9.5 ± 1.8	9.0 ± 1.1
Duration of diabetes (years)	10.0 ± 8.8	9.3 ± 8.4	11.0 ± 9.5
Treatment			
Diet (kcal/SBW/day)	29.4 ± 2.8	29.4 ± 3.0	29.4 ± 2.5
Medications			
Ins only (n)	28	15	13
Ins + Met (n)	2	1	1
Ins + SU (n)	2	2	0
SU (n)	13	9	4
SU + Met (n)	4	4	0
Met only (n)	3	1	2
None (n)	8	4	4

Data are means ± SD. BMI, body mass index; BEE, basal energy expenditure; FPG, fasting plasma glucose just before the measurement of BEE; PPPG, mean preprandial plasma glucose for three consecutive days before the measurement of BEE; HbA1c, glycated hemoglobin; SBW, standard body weight; Ins, insulin; SU, sulfonylurea; Met, metformin.

There are potential weaknesses of the present study. First, only a small number of patients with type 1 diabetes was included. However, no difference in the value of BEE between patients with type 1 and type 2 diabetes has been described to date. In type 1 diabetes, the elevated energy expenditure is observed only during insulin deprivation, and it returns to normal level by insulin treatment.[28] In type 2 diabetes, there is no difference in FFM-adjusted REE between mildly hyperglycemic patients and controls.[6] Thus, when they are under treatment, BEE in both type 1 and type 2 diabetes patients can be assumed comparable to that in healthy people. In addition, our validation data set has more background in common with the derivation set than the general population of Japanese patients with diabetes. We also did not measure BEE of healthy Japanese for comparison. It remains to be established whether or not the difference in BEE between Japanese patients with diabetes and healthy Japanese is insignificant when FPG of patients are <180 mg/dL.

The values estimated from the proposed equation in the present study are well matched to the reference values for Japanese BEE (Dietary reference intakes) reported in healthy Japanese as values per body weight among different groups for age and sex.[29] In addition, when mean BEE values were calculated by the proposed equation from mean body weight and age reported in other studies including healthy Japanese and Chinese, estimated BEE values were in good agreement with measured values.[10,15,30]

We report a new equation using parameters readily available in clinical practice to estimate BEE of patients with diabetes in an Asian population. Further studies are required to in a wide range of populations to determine its usefulness in Asian clinical settings.

Table 7
Evaluation of equations in validation set.

Equation	Estimated BEE per body[a]	Estimated BEE per kg Wt[b]	Bias[c]	RMSE[d]	Accurate estimation[e]
New equation	1317 ± 227	20.2 ± 2.3	4.8 ± 7.7	103	78
Harris and Benedict	1388 ± 309	21.1 ± 2.2	9.8 ± 9.4	184	50
Oxford	1420 ± 309	21.6 ± 2.3	12.3 ± 9.5	209	38
Liu	1407 ± 321	21.3 ± 2.1	11.1 ± 10.9	205	42
Ganpule	1323 ± 295	20.1 ± 2.4	4.5 ± 10.5	140	63

n = 60. Data are means ± SD.
[a] Estimated BEE per body, mean basal energy expenditure estimated per body (kcal/day).
[b] Estimated BEE per kg Wt, mean basal energy expenditure estimated per kg body weight (kcal/kg/day).
[c] Bias, mean percentage error between estimated and measured BEE ((BEE estimated − BEE measured)/BEE measured) (%).
[d] RMSE, root mean squared error (kcal/day).
[e] Accurate estimation, percent of the patients estimated by each equation within ±10% of measured value (%).

Statement of authorship

The authors' responsibilities were as follows: KI, SF, MG, and TK designed research; KI, CY, AH, MI, KN and KS conducted research; KI, MG, and SF analyzed data; KI and SF wrote the paper; and NI supervised research. All authors read and approved the final manuscript.

Conflict of interest

None of the authors had any conflict of interest.

Acknowledgements

This study was supported by a research grant from the Ministry of Health, Labour and Welfare of Japan and also by Kyoto University Global COE program "Center for Frontier Medicine".

The authors thank Masayuki Yokode from Kyoto University Hospital Translational Research Center Department of Clinical Innovative Medicine for his general assistance in conducting this research.

References

1. American Diabetes Association. Nutrition recommendations and interventions for diabetes: a position statement of the American Diabetes Association. *Diabetes Care* 2008;**31**(Suppl. 1):S61–78.
2. Cunningham JJ. Body composition as a determinant of energy expenditure: a synthetic review and a proposed general prediction equation. *Am J Clin Nutr* 1991;**54**:963–9.
3. Bitz C, Toubro S, Larsen TM, Harder H, Rennie KL, Jebb SA, et al. Increased 24-h energy expenditure in type 2 diabetes. *Diabetes Care* 2004;**27**:2416–21.
4. Martin K, Wallace P, Rust PF, Garvey WT. Estimation of resting energy expenditure considering effects of race and diabetes status. *Diabetes Care* 2004;**27**:1405–11.
5. Ikeda K, Fujimoto S, Goto M, Yamada C, Hamasaki A, Shide K, et al. Impact of endogenous and exogenous insulin on basal energy expenditure in patients with type 2 diabetes under standard treatment. *Am J Clin Nutr* 2011;**94**:1513–8.
6. Ryan M, Sallé A, Guilloteau G, Genaitay M, Livingstone MB, Ritz P. Resting energy expenditure is not increased in mildly hyperglycaemic obese diabetic patients. *Br J Nutr* 2006;**96**:945–8.
7. Harris JA, Benedict FG. *A biometric study of basal metabolism in man*. Washington, DC: Carnegie Institute of Washington; 1919 [Publication number 297].
8. Leung R, Woo J, Chan D, Tang N. Validation of prediction equations for basal metabolic rate in Chinese subjects. *Eur J Clin Nutr* 2000;**54**:551–4.
9. Case KO, Brahler CJ, Heiss C. Resting energy expenditures in Asian women measured by indirect calorimetry are lower than expenditures calculated from prediction equations. *J Am Diet Assoc* 1997;**97**:1288–92.
10. Liu H-Y, Lu Y-F, Chen W-J. Predictive equations for basal metabolic rate in Chinese adults: a cross-validation study. *J Am Diet Assoc* 1995;**95**:1403–8.
11. Henry CJK, Rees DG. New predictive equations for the estimation of basal metabolic rate in tropical peoples. *Eur J Clin Nutr* 1991;**45**:177–85.
12. Cole TJ, Henry CJK. The Oxford Brookes basal metabolic rate database—a reanalysis. *Public Health Nutr* 2005;**8**:1202–12.
13. Wouters-Adeiaens MPE, Westerterp KR. Low resting energy expenditure in Asians can be attributed to body composition. *Obesity* 2008;**16**:2212–6.

14. Soares MJ, Piers LS, O'Dea K, Shetty PS. No evidence for an ethnic influence on basal metabolism: an examination of data from India and Australia. *Br J Nutr* 1998;**79**:333–41.
15. Miyake R, Tanaka S, Ohkawara K, Ishikawa-Takata K, Hikihara Y, Taguri E, et al. Validity of predictive equations for basal metabolic rate in Japanese adults. *J Nutr Sci Vitaminol* 2011;**57**:224–32.
16. Bursztein S, Elwyn DH, Askanazi J, Kinney JM. *Energy metabolism, indirect calorimetry, and nutrition*. Baltimore: Lippincott Williams & Wilkins; 1989.
17. Compher C, Frankenfield D, Keim N, Roth-Yousey L. Evidence analysis working group. Best practice methods to apply to measurement of resting metabolic rate in adults: a systematic review. *J Am Diet Assoc* 2006;**106**:881–903.
18. Frary CD, Johnson RK. Energy. In: Mahan LK, Escott-Stump S, editors. *Krause's food & nutrition therapy*. 12th ed. 2007. p. 22–38.
19. Japan Diabetes Society. *Treatment guide for diabetes*. Tokyo Japan: Bunkodo; 2007.
20. Weir JB. New methods for calculating metabolic rate with special reference to protein metabolism. *J Physiol* 1949;**109**:1–9.
21. Japanese anthropometric reference data. *Jpn J Nutr Assesment* 2002;**19**:12–9.
22. The Committee of the Japan Diabetes Society on the diagnostic criteria of diabetes mellitus. Report of the committee on the classification and diagnostic criteria of diabetes mellitus. *J Diabetes Invest* 2010;**1**:212–28.
23. Weijs PJM, Vansant GAAM. Validity of predictive equations for resting energy expenditure in Belgian normal weight to morbid obese women. *Clin Nutr* 2010;**29**:347–51.
24. Nelson KM, Weinsier RL, Long CL, Schutz Y. Prediction of resting energy expenditure from fat-free mass and fat mass. *Am J Clin Nutr* 1992;**56**: 848–56.
25. Lean MEJ, Han TS, Deurenberg P. Predicting body composition by densitometry from simple anthropometric measurements. *Am J Clin Nutr* 1996;**63**:4–14.
26. Johnstone AM, Rance KA, Murison SD, Duncan JS, Speakman JR. Additional anthropometric measures may improve the predictability of basal metabolic rate in adult subjects. *Eur J Clin Nutr* 2006;**60**:1437–44.
27. Korth O, Bosy-Westphal A, Zschoche P, Glüer CC, Heller M, Müller MJ. Influence of methods used in body composition analysis on the prediction of resting energy expenditure. *Eur J Clin Nutr* 2007;**61**:582–9.
28. Hebert SL, Nair KS. Protein and energy metabolism in type 1 diabetes. *Clin Nutr* 2010;**29**:13–7.
29. Ministry of Health, Labour and Welfare of Japan. *Dietary reference intakes for Japanese, 2010*. Tokyo, Japan: Daiichi Shuppan; 2009.
30. Usui C, Takahashi E, Gando Y, Sanada K, Oka J, Miyachi M, et al. Resting energy expenditure can be assessed by dual-energy X-ray absorptiometry in women regardless of age and fitness. *Eur J Clin Nutr* 2009;**63**:529–35.

Reduction of Reactive Oxygen Species Ameliorates Metabolism-Secretion Coupling in Islets of Diabetic GK Rats by Suppressing Lactate Overproduction

Mayumi Sasaki,[1] Shimpei Fujimoto,[1,2] Yuichi Sato,[1] Yuichi Nishi,[1,2] Eri Mukai,[1] Gen Yamano,[1] Hiroki Sato,[1] Yumiko Tahara,[1] Kasane Ogura,[1] Kazuaki Nagashima,[1] and Nobuya Inagaki[1]

We previously demonstrated that impaired glucose-induced insulin secretion (IS) and ATP elevation in islets of Goto-Kakizaki (GK) rats, a nonobese model of diabetes, were significantly restored by 30–60-min suppression of endogenous reactive oxygen species (ROS) overproduction. In this study, we investigated the effect of a longer (12 h) suppression of ROS on metabolism-secretion coupling in β-cells by exposure to tempol, a superoxide (O_2^-) dismutase mimic, plus ebselen, a glutathione peroxidase mimic (TE treatment). In GK islets, both H_2O_2 and O_2^- were sufficiently reduced and glucose-induced IS and ATP elevation were improved by TE treatment. Glucose oxidation, an indicator of Krebs cycle velocity, also was improved by TE treatment at high glucose, whereas glucokinase activity, which determines glycolytic velocity, was not affected. Lactate production was markedly increased in GK islets, and TE treatment reduced lactate production and protein expression of lactate dehydrogenase and hypoxia-inducible factor 1α (HIF1α). These results indicate that the Warburg-like effect, which is characteristic of aerobic metabolism in cancer cells by which lactate is overproduced with reduced linking to mitochondria metabolism, plays an important role in impaired metabolism-secretion coupling in diabetic β-cells and suggest that ROS reduction can improve mitochondrial metabolism by suppressing lactate overproduction through the inhibition of HIF1α stabilization. ***Diabetes* 62:1996–2003, 2013**

In pancreatic β-cells, intracellular glucose metabolism regulates the exocytosis of insulin granules according to metabolism-secretion coupling in which ATP production in mitochondria plays an essential role (1). The reduction of mitochondrial ATP production causes the impairment of glucose-induced IS in various conditions (2).

Reactive oxygen species (ROS) such as superoxide (O_2^-) and hydrogen peroxide (H_2O_2) are normal byproducts of glucose metabolism, including glycolysis and mitochondrial oxidative phosphorylation (3). In pancreatic β-cells, ROS production via nonmitochondrial and mitochondrial pathways has been proposed. In the mitochondrial pathway, ROS is generated in the electron transport chain associated with the mitochondrial membrane potential (4). However, in pathophysiological conditions, NADPH oxidase, an important nonmitochondrial ROS source, may play an important role in ROS generation in β-cells (5). Antioxidant capacity in β-cells is very low because of weak expression of antioxidant enzymes such as catalase, glutathione peroxidase (GPx), and O_2^- dismutase (SOD) in pancreatic islets compared with that in various other tissues (6,7), which suggests vulnerability of β-cells to ROS. Gene expression profiling in islets revealed that SOD, which metabolizes O_2^- to H_2O_2, was 30–40% and GPx, which metabolizes H_2O_2 to H_2O, was 15% of that in liver. Moreover, catalase was not detectable in islets (7).

In β-cells, ROS is one of the most important factors that impair metabolism-secretion coupling (1). Exposure to exogenous H_2O_2, the most abundant ROS, reduces glucose-induced IS by impairing mitochondrial metabolism in β-cells (8). We have proposed that endogenous overproduction of ROS that involves the activation of Src, a nonreceptor tyrosine kinase, plays an important role in impaired metabolism-secretion coupling in islets of diabetic Goto-Kakizaki (GK) rats (9–11). The suppression of the overproduction of ROS for 30–60 min by exposure to ROS scavengers and by suppression of Src activity restores impaired glucose-induced IS and ATP elevation in GK rat islets (9,10). However, the effect of reducing the overproduction of ROS for a longer duration on impaired metabolism-secretion coupling in diabetic β-cells remains unknown.

In the current study, we investigated the effects of 12-h suppression of endogenous ROS production on impaired metabolism-secretion coupling in β-cells by exposing cell-permeable antioxidant enzyme mimics, including tempol, an SOD mimic (12), and ebselen, a GPx mimic (13), which are commonly used in the field of diabetology without cytotoxic effects (14,15). Our results indicate that 12-h suppression of ROS improves metabolism-secretion coupling by a mechanism different from that involved in improvement by ROS reduction for 30–60 min.

From the [1]Department of Diabetes and Clinical Nutrition, Graduate School of Medicine, Kyoto University, Kyoto, Japan; and the [2]Department of Endocrinology, Metabolism, and Nephrology, Kochi Medical School, Kochi University, Nankoku, Japan.
Corresponding author: Nobuya Inagaki, inagaki@metab.kuhp.kyoto-u.ac.jp.
Received 6 July 2012 and accepted 22 December 2012.
DOI: 10.2337/db12-0903
This article contains Supplementary Data online at http://diabetes.diabetesjournals.org/lookup/suppl/doi:10.2337/db12-0903/-/DC1.

See accompanying commentary, p. 1823.

RESEARCH DESIGN AND METHODS

Materials. Ebselen was purchased from Calbiochem (La Jolla, CA). HEPES, KCl, EGTA, glucose, NaCl, $NaHCO_3$, $HClO_4$, Na_2CO_3, H_2O_2, BSA, and the substrates used in ATP production, except glycerol phosphate, were purchased from Nacalai (Kyoto, Japan). [U-^{14}C]-glucose was obtained from GE Healthcare (Uppsala, Sweden). Lactate dehydrogenase (EC 1.1.1.27) and Dowex 1 × 8 anion exchange resin (formate) (50–100 mesh) were obtained from Wako (Osaka, Japan). Hypoxia-inducible factor 1α (HIF1α) inhibitor (3-[2-(4-adamantan-1-yl-phenoxy)-acetylamino]-4-hydroxybenzoic acid methyl ester) was obtained from Merck Millipore (Darmstadt, Germany). All other reagents were obtained from Sigma-Aldrich (St. Louis, MO).

Animals. Male Wistar and GK rats were obtained from Shimizu (Kyoto, Japan). All experiments were carried out with rats 7–10 weeks of age. The body weight

of GK rats used in the experiments was similar to that of Wistar rats (means ± SE; Wistar, 231 ± 3, vs. GK, 217 ± 3 g, not significant). The nonfasting plasma glucose of GK rats was higher compared with that of Wistar rats (means ± SE; Wistar, 5.72 ± 0.12, vs. GK, 11.57 ± 0.58 mmol/L, $P < 0.01$). The animals were maintained and used in accordance with the guidelines of the animal care committee of Kyoto University.

Islet isolation and culture. Pancreatic islets were isolated from Wistar and GK rats by collagenase digestion as described previously (16). Isolated islets were washed with Krebs-Ringer bicarbonate buffer (KRBB) containing 2.8 mmol/L glucose and cultured for 12 h in RPMI-1640 medium containing 10% FCS and 5.5 mmol/L glucose without or with 10 mmol/L tempol, 10 μmol/L ebselen, or combination of tempol and ebselen (TE treatment) at 37°C in humidified air containing 5% CO_2. Insulin content of GK islets was similar to that of Wistar islets (means ± SE; Wistar, 20.0 ± 2.2, vs. GK, 23.0 ± 2.6 ng/islet, not significant).

Measurement of O_2^- and H_2O_2 generations. O_2^- and the H_2O_2 production were measured at the end of the 12-h culture in conditions described above. O_2^- generation was detected by nitroblue tetrazolium (NBT) assay (17) using KRBB supplemented with 0.2% BSA (fraction V) and 10 mmol/L HEPES adjusted to pH 7.4 (KRBB medium). Groups of 100 islets were batch incubated in tubes containing 0.5 mL KRBB medium supplemented with 5.5 mmol/L glucose with 0.2% (weight/volume) NBT at 37°C for 30 min. After the islets were centrifuged (1,000 rpm for 2 min at 4°C), the supernatant was removed and formazan-NBT (NBT reduced) was dissolved in 100 μL 50% (volume/volume) acetic acid by sonication (5-s pulse, five times). The sonicate was briefly centrifuged, and the absorbance of the supernatant was measured at 560 nm using a spectrofluorometer (Shimadzu RF-5000, Kyoto, Japan). H_2O_2 release from islets was measured according to the method previously described (18). In brief, islets were cultured for 12 h in various conditions as described above. Groups of 150 islets were batch incubated for 60 min in KRBB medium containing 5.5 mmol/L glucose with 0.1 mg/mL horseradish peroxidase (type II) and 0.44 mmol/L homovanillic acid. After the islets were centrifuged (1,000 rpm for 2 min at 4°C), the supernatant was removed. Fluorescence of the supernatant was measured at excitation and emission of 315 and 425 nm, respectively, using a spectrofluorometer (Shimadzu RF-5000). Standard curves were produced using samples containing known amounts of H_2O_2 without islets.

Measurement of insulin release, ATP contents, and glucose oxidation. Insulin release from islets was monitored using batch incubation as described previously (16). ATP content in islets was determined as previously described (9). ATP contents were measured using ENLITEN luciferin-luciferase solution (Promega, Madison, WI) by luminometer (GloMax 20/20n; Promega). Glucose oxidation was carried out using the previously described method (19).

Intraperitoneal glucose tolerance tests. After GK rats were divided into two groups, one group received intraperitoneal injection of tempol (50 mg/kg) and ebselen (10 mg/kg) twice (12 and 6 h before intraperitoneal glucose tolerance tests [ip-GTTs]) during a 15-h fast (TE); the other group was treated similarly with vehicle alone. After these treatments, ip-GTTs (1 g/kg body weight) were performed. Plasma glucose and plasma insulin levels were measured in samples taken at the indicated times. Plasma glucose levels were determined by the glucose oxidase method. Plasma insulin levels were determined using an enzyme immunoassay (Shibayagi, Gunma, Japan).

Immunoblot analysis. The preparations for whole-islet lysate and for the mitochondrial fraction were described previously (20,21). Western blotting was performed as previously described (20) with the following antibodies: mouse monoclonal anti–complex I (39 kDa subunit), anti–complex III (core II),

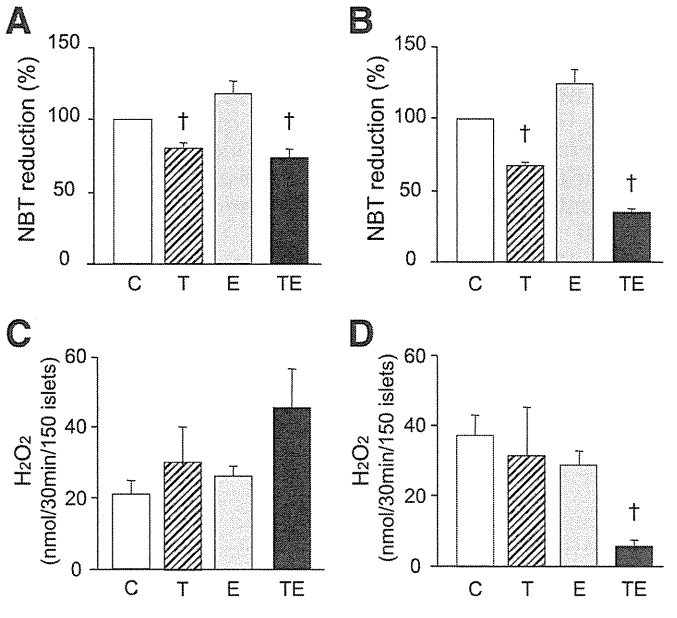

FIG. 1. Effects of antioxidant enzyme mimics on ROS production in Wistar (*A* and *C*) and GK (*B* and *D*) islets. Islets were isolated and cultured without (control [C]; white bars) or with 10 mmol/L tempol (T; hatched bars), 10 μmol/L ebselen (E; gray bars), or T plus E (TE; black bars). O_2^- generation (*A* and *B*) was determined by measuring the reduction of NBT using 100 islets, and data were shown as fold increase relative to control. H_2O_2 generation (*C* and *D*) was determined by measuring the peroxidation of homovanillic acid included in the reaction mixtures as a substrate using 150 islets. Data are shown as means ± SE of three different experiments. †$P < 0.01$ vs. control.

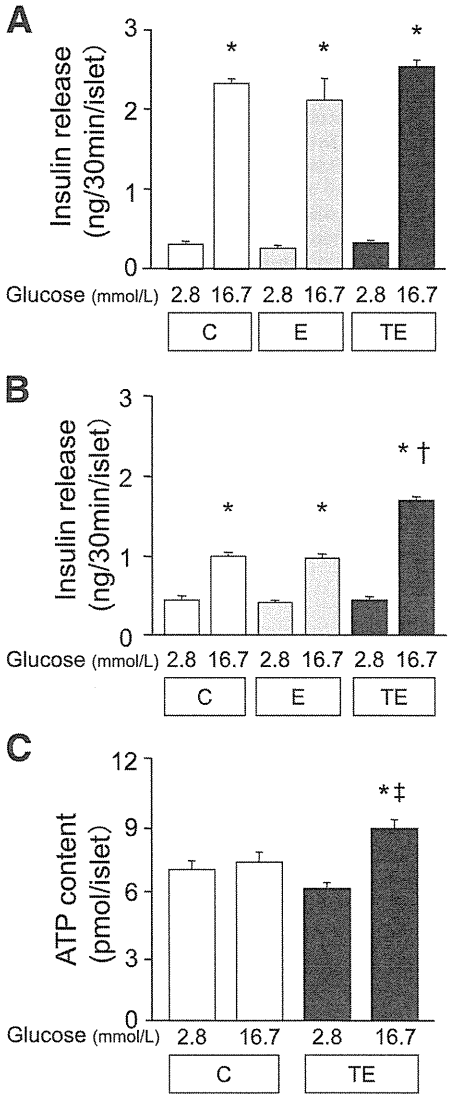

FIG. 2. Effects of antioxidant enzyme mimics on IS (*A* and *B*) and ATP contents (*C*). Islets were cultured without (control [C]) or with ebselen (E; gray bars) and tempol plus ebselen (TE; black bars) for 12 h. After cultured islets were washed and preincubated with 2.8 mmol/L glucose for 30 min, islets were incubated for 30 min at 2.8 and 16.7 mmol/L glucose, and released insulin was measured. Insulin release from Wistar islets (*A*) and in GK islets (*B*) is shown. After cultured GK islets were washed and preincubated with 2.8 mmol/L glucose for 30 min, islets were incubated for 30 min at 2.8 and 16.7 mmol/L glucose, and ATP contents in GK islets were measured (*C*). Data are expressed as the mean ± SE of 25 (*A* and *B*) or 20 (*C*) determinations from three (*A* and *C*) and four (*B*) experiments. *$P < 0.01$ vs. corresponding 2.8 mmol/L glucose; †$P < 0.01$ vs. 16.7 mmol/L glucose in control; ‡$P < 0.05$ vs. 16.7 mmol/L glucose in control.

anti–complex IV (subunit I), and anti–complex V (subunit α) of the mitochondrial respiratory chain (1:1,000) from Invitrogen (Carlsbad, CA), mouse anti–β-actin (1:5,000) from Sigma-Aldrich, rabbit polyclonal anti–LDH-A (1:1,000) from Cell Signaling (Danvers, MA), rabbit anti–PDK-1 (1:1,000) and rabbit anti-HIF1α (1:250) from Abcam (Paris, France), rabbit anti-UCP2 (1:200) from Chemicom (Temecula, CA), mouse anti–hsp-60 (1:5,000) from BD Biosciences (Franklin Lakes, NJ), rabbit anti–PK-M2 (1:2,500) from Novus Biological, LLC (Littleton, CO), and horseradish peroxidase–conjugated anti-rabbit and -mouse antibody (1:5,000) from GE Healthcare. Proteins were detected using an enhanced chemiluminescence system (GE Healthcare). Protein density was quantified by densitometric analysis using Multi Gauge software (Fujifilm, Tokyo, Japan).

Measurements of enzyme activities. After islets were cultured with or without TE for 12 h, whole-islet homogenates and mitochondrial fractions from cultured islets were obtained. Glucokinase and hexokinase activities were determined using whole-islet homogenates by NADH formation in an enzyme reaction as previously described (22). The activity of mitochondrial glycerol phosphate dehydrogenase (mGPDH) in whole-islet homogenates of Wistar and GK rats was measured by the reduction of 2-*p*-iodo-3-*p*-nitro-5-phenyltetrezolium to indoformazan as previously described (23). The activity of mGPDH in the mitochondrial fraction from GK islets was measured by the method based on the generation of ^{3}HOH from L-[2-^{3}H]glycerol-3-phosphate (24). In brief, after mitochondrial fractions were incubated at 37°C for 30 min with 2.5 mCi/mmol L-[2-^{3}H] glycerol-3-phosphate and the reaction was stopped by the addition of antimycin A, the mixture was immediately applied to a column of Dowex 1-X8 (formate), which was washed with 0.5 mL water. The radioactivity of the column effluent was measured by a liquid scintillation counter.

Measurement of mitochondrial ATP production. The mitochondrial fraction from islets and measurement of ATP production were performed as previously described (21).

Measurement of lactate production. Lactate production was measured as previously described (25). In brief, after preincubation, groups of 20 islets were batch incubated in KRBB medium containing 2.8 and 16.7 mmol/L glucose for 60 min at 37°C. The supernatant (200 μL) was mixed with 0.5 mL of 0.5 mol/L glycine/0.4 mol/L hydrazine buffer (pH 9.0) containing 2.4 mmol/L NAD and 7.2 units/mL lactate dehydrogenase, and was incubated for 30 min at 37°C. The fluorescence of NADH was then measured at an excitation of 340 nm and emission of 450 nm. Standard curves were produced from samples containing known amounts of lactate.

Statistical analysis. The data are expressed as means ± SE. Statistical significance was determined by unpaired Student *t* test. $P < 0.05$ was considered significant.

RESULTS

O_2^- and H_2O_2 production during culture with antioxidant mimics. Tempol, an SOD mimic, decreased O_2^- production in Wistar (Fig. 1*A*) and GK islets (Fig. 1*B*) but had no effect on H_2O_2 production in either of the islets (Fig. 1*C* and *D*). Ebselen, a GPx mimic, had no reducing effect on O_2^- and H_2O_2 production in either of the islets (Fig. 1). Cotreatment with TE reduced O_2^- production by 27.0% but had no effect on H_2O_2 production in Wistar islets (Fig. 1*A* and *C*). On the other hand, in GK islets, TE treatment prominently reduced O_2^- and H_2O_2 production by 65.0 and 84.6%, respectively (Fig. 1*B* and *D*). Taken together, these findings indicate that TE treatment is effective in reducing oxidative stress in GK islets.

Effect of TE treatment on IS. The effect of antioxidant mimics on β-cell function was investigated. In the presence of 16.7 mmol/L glucose, insulin secretion (IS) from GK islets was reduced compared with that from control Wistar rats (GK, 1.01 ± 0.06, vs. Wistar, 2.32 ± 0.11 ng/30 min/islet, $P < 0.01$). Although TE treatment had no effect on IS from Wistar islets (Fig. 2*A*), it restored high glucose–induced IS (Fig. 2*B*) and ATP content (Fig. 2*C*) in GK islets. We demonstrated previously that impaired glucose-induced IS in GK islets was significantly restored by acute exposure to PP2, a Src inhibitor (9). To examine the involvement of Src inhibition in the improvement of glucose-induced IS after TE treatment, TE-treated GK islets were incubated for 30 min with or without 10 μmol/L PP2 in the presence of 16.7 mmol/L glucose. In TE-treated GK islets, 30-min exposure to PP2 prominently enhanced IS at high glucose (control, 1.71 ± 0.07, vs. PP2, 4.06 ± 0.22 ng/30 min/islet, $P < 0.01$), which implies involvement of an independent mechanism of Src inhibition in the improvement of glucose-induced IS by chronic TE treatment.

To investigate the effects of TE treatment on β-cell function in vivo, a GTT was assessed after intraperitoneal TE administration (Table 1). In GK rats, TE treatment decreased the glucose level at 15 and 30 min and increased insulin levels at 30 min after glucose loading. Studies using isolated islets from GK rats after TE treatment in vivo revealed that high glucose–induced IS was increased by TE treatment (Table 2).

Effect of TE treatment on expression of UCP2 and mitochondrial respiratory chain proteins. Immunoblot analysis showed that TE treatment had no effect on protein levels of UCP2 in protein extracts of the islet mitochondrial fraction (Supplementary Fig. 1*A*) and on those of complex I, III, IV, and V of the mitochondrial respiratory chain in lysates of whole islets (Supplementary Fig. 1*B*) in both GK and Wistar islets.

Effect of TE treatment on glucose metabolism. TE treatment had no effect on glucokinase and hexokinase activities, which determines the velocity of glycolysis in β-cells (26), in GK and Wistar islets (Table 3). By TE treatment, glucose oxidation at high glucose, an indicator of Krebs cycle velocity, was not affected in Wistar islets, whereas it was significantly increased in GK islets (control, 25.4 ± 4.1, vs. TE, 55.8 ± 12.2 pmol/islet/90 min, $P < 0.05$) (Fig. 3).

Effect of TE treatment on ATP production and on activity of mGPDH. ATP production by mitochondria from control and TE-treated islets of Wistar and GK rats was measured in the presence of various substrates and inhibitors (Table 4), including succinate (electron transfer at complex I by NADH generation in the Krebs cycle and at complex II directly), succinate with rotenone (electron

TABLE 1
Ip-GTT in GK rats treated with TE in vivo

		Minute				
		0	15	30	60	120
Glucose (mg/dL)	Control	145 ± 4	475 ± 6	423 ± 11	340 ± 14	184 ± 7
	TE	144 ± 11	330 ± 41†	359 ± 28*	330 ± 24	200 ± 13
Insulin (pg/mL)	Control	164 ± 70	ND	172 ± 50	ND	205 ± 75
	TE	205 ± 32	ND	400 ± 101*	ND	209 ± 46

After the intraperitoneal injection of 50 mg/kg tempol plus 10 mg/kg ebselen (TE) or vehicle alone (control) twice during a 15-h fast in GK rats, GTT with intraperitoneal injection of glucose (1 g/kg body weight) was performed and plasma glucose and insulin levels were measured. Data are means ± SE of seven independent experiments. ND, not determined. *$P < 0.05$ vs. corresponding control TE. †$P < 0.01$ vs. corresponding control without TE.

TABLE 2
Insulin secretion from isolated islets in GK rats treated with tempol plus ebselen in vivo

	2.8 mmol/L glucose	16.7 mmol/L glucose
Control (ng/30 min/islet)	0.40 ± 0.04	0.84 ± 0.06
TE (ng/30 min/islet)	0.49 ± 0.04	1.42 ± 0.13*

After the intraperitoneal injection of 50 mg/kg tempol plus 10 mg/kg ebselen (TE) or vehicle alone (control) twice during a 15-h fast in GK rats, islets were isolated and IS in the presence of 2.8 and 16.7 mmol/L glucose was measured. Data are means ± SE of nine determinations. *$P < 0.01$ vs. corresponding control without TE.

transfer at complex II and inhibition of electron transfer through NADH at complex I), glutamate plus malate (electron transfer mainly at complex I by NADH generation derived from reaction via glutamate dehydrogenase), pyruvate plus malate (electron transfer mainly at complex I by NADH generation derived from reaction via pyruvate dehydrogenase), ascorbate plus N,N,N′,N′-tetramethyl-p-phenylenediamine (TMPD) (electron transfer at complex IV directly), and glycerol-3-phosphate (G3P) (electron transfer at complex II by $FADH_2$ generation derived from reaction via mGPDH). Control and TE-treated mitochondria showed similar rates of ATP production for all substrates tested, except for G3P. TE treatment promotes the rate of mitochondrial ATP production in the presence of G3P in Wistar and GK islets 3.3- and 2.2-fold, respectively. In the measurement of activity of mGPDH using whole islet homogenates, the value in GK islets was lower compared with that of Wistar islets, and enhancement of the activity by TE treatment was not significant in either Wistar or GK islets (Table 3). However, in the measurement of activity of mGPDH using intact mitochondria, TE treatment increased mGPDH activity in GK mitochondria (Table 3).

Lactate production and protein expression of lactate dehydrogenase and HIF1α. Lactate production in GK islets was significantly higher compared with that in Wistar islets at both basal and stimulated levels of glucose (at 2.8 mmol/L glucose: Wistar, 1.32 ± 0.15, vs. GK, 8.15 ± 1.36, $P < 0.01$; at 16.7 mmol/L glucose: Wistar, 3.09 ± 0.33, vs. GK, 14.08 ± 1.68, $P < 0.01$) (Fig. 4*A*). TE treatment suppressed lactate production at both basal and stimulated levels of glucose in both Wistar and GK islets; the most prominent reduction in these conditions was at 16.7 mmol/L glucose in GK islets (control, 14.08 ± 1.68, vs. TE, 5.71 ± 0.79, $P < 0.01$). Protein expression levels of HIF1α, a potential upstream regulator of lactate dehydrogenase (LDH), in INS-1 cells were gradually increased over 12 h in the presence of 200 μmol/L $CoCl_2$, a chemical inducer of HIF1α (27) (Supplementary Fig. 2). TE treatment time-dependently suppressed HIF1α levels in GK islets, and the reduction was significant after 9-h TE treatment (~30% reduction at 9 h; ~50% reduction at 12 h) (Fig. 4*B*). Protein expression levels of HIF1α and HIF1α downstream targets, including LDH-A and pyruvate dehydrogenase-1 (PDK-1), were examined 12 h after TE treatment. In GK islets, TE treatment significantly decreased HIF1α, LDH-A, and M2-PK expression (HIF1α, ~50% reduction; LDH-A, ~30% reduction; M2-PK, ~30% reduction) but did not affect PDK-1 expression (Fig. 4*C* and Supplementary Fig. 3).

Effect of HIF1α inhibitor on IS and lactate production in GK islets. IS in the presence of 16.7 mmol/L glucose from GK islets was enhanced by HIF1α inhibitor treatment (control, 1.34 ± 0.07, vs. HIF1α inhibitor, 1.77 ± 0.09 ng/30 min/islet, $P < 0.01$). Lactate production in the presence of 2.8 and 16.7 mmol/L glucose was reduced by HIF1α inhibitor treatment (2.8 mmol/L glucose: control, 12.44 ± 1.12, vs. HIF1α inhibitor, 9.46 ± 0.89 pmol/islet, $P < 0.01$; 16.7 mmol/L glucose: control, 15.39 ± 1.02, vs. HIF1α inhibitor, 12.42 ± 1.40 pmol/islet, $P < 0.01$) (Fig. 5).

DISCUSSION

The current study demonstrates that combination treatment by tempol, an SOD mimic, and ebselen, a GPx mimic (TE treatment), efficiently suppressed both H_2O_2 and O_2^- production in GK islets. Moreover, impaired glucose-induced IS and ATP elevation in GK islets were significantly improved by TE treatment but were not improved by tempol or ebselen alone. These results are compatible with previous studies in which coexpression of the antioxidant enzymes in a β-cell line was more efficient than expression of either single enzyme in reducing ROS production and oxidative injury (7,28,29).

We then examined the precise mechanisms of the improvement in glucose-induced ATP elevation in GK islets by TE treatment. UCP2 decreases mitochondrial ATP production by reducing mitochondrial hyperpolarization derived from an increase in mitochondrial proton conductance. UCP2 negatively regulates metabolism-secretion

TABLE 3
Effect of TE treatment on glucokinase, hexokinase, and mitochondrial G3P dehydrogenase activities

Experimental conditions		Wistar rat	GK rat
Hexokinase (whole islet extracts)	Control	21.58 ± 3.23	131.46 ± 23.62
(pmol/islet/h)	TE	21.63 ± 3.18	138.19 ± 35.97
Glucokinase (whole islet extracts)	Control	22.79 ± 8.21	52.71 ± 8.82
(pmol/islet/h)	TE	22.90 ± 6.53	42.41 ± 8.96
mGPDH (whole islet extracts)	Control	9.90 ± 0.34	6.76 ± 0.32*
(nmol/mg protein/min)	TE	10.60 ± 0.75	7.37 ± 0.14
mGPDH (mitochondrial fraction)	Control	ND	65.77 ± 1.61
(nmol/mg mitochondrial protein/min)	TE	ND	75.41 ± 2.34†

After islets were cultured with or without TE for 12 h, extract from whole islets and mitochondrial fractions were obtained. Data are given as the mean ± SE from five experiments for glucokinase and hexokinase, six experiments for mGPDH using whole-islet extracts, and three experiments for mGPDH using the mitochondrial fraction. ND, not determined. *$P < 0.05$ vs. Wistar control without TE. †$P < 0.05$ vs. control without TE.

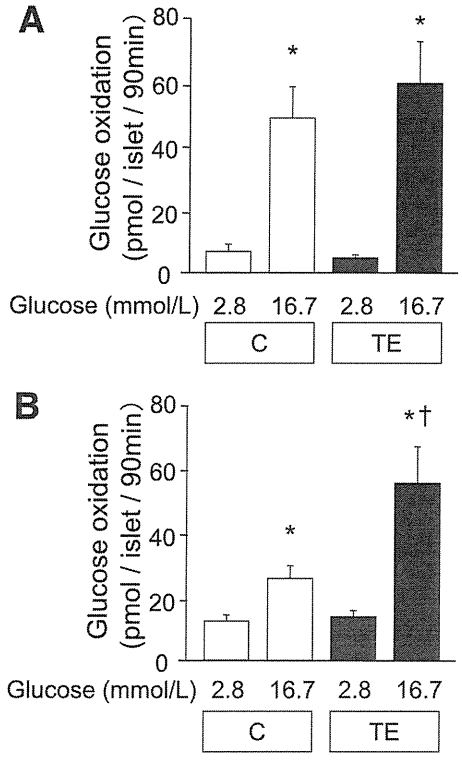

FIG. 3. Effects of TE treatment on glucose oxidation in Wistar (*A*) and GK (*B*) islets. Islets were cultured without (control [C]; open bars) or with TE (black bars) for 12 h. After cultured islets were preincubated with 2.8 mmol/L glucose for 30 min, glucose oxidation during incubation for 90 min in the presence of 2.8 and 16.7 mmol/L glucose was measured in islets. Data are shown as means ± SE of 12 determinations from three (A) and four (B) experiments. *$P < 0.01$ vs. corresponding 2.8 mmol/L glucose; †$P < 0.01$ vs. 16.7 mmol/L glucose in control.

coupling in β-cells (30,31). However, regulation of UCP2 expression may not play an important role in the mechanism, as the UCP2 expression level was not affected in GK islets by TE treatment. Western blot analysis revealed that the expression of respiratory chain proteins, including complex I, III, IV, and V, was not affected by TE treatment. In addition, the relative mRNA levels of nuclear factors, including *NRF-1*, *NRF-2*, and *TFAM*, which affect mitochondrial biogenesis, also were not altered by TE treatment (data not shown). These results indicate that the regulation of mitochondrial mass is not involved in the mechanism.

ATP production is driven by the H^+ gradient across the mitochondrial membrane generated by the transport of high-energy electrons in the respiratory chain. These electrons are derived from NADH and $FADH_2$, derived from the Krebs cycle in the matrix and/or transferred from the cytosol by the shuttle system. To determine which step in mitochondrial carbohydrate metabolism is affected in TE-treated islets, ATP production in the presence of various substrates and inhibitors was measured using mitochondrial fractions from the cultured islets. In the presence of G3P, ATP production was increased by TE treatment in both the Wistar and GK mitochondrial fraction. Transfer of a reduced equivalent from cytosol to mitochondria by the glycerol phosphate shuttle may well play a more important role in mitochondrial ATP production in islets than in other tissues, since the activity of mGPDH, a key enzyme in the glycerol phosphate shuttle is ~60-fold higher in islets than in other tissues (24). In addition, decreased activity is observed in diabetic islets (32). Although an increase in the activity of mGPDH by TE treatment was detected, the increase was similar in the mitochondrial fraction from both GK and Wistar islets. Therefore, an improvement of mGPDH activity alone may not account for the improvement in glucose-induced ATP elevation in GK islets by TE treatment.

TE treatment did not affect the activity of glucokinase, a rate-limiting enzyme in glycolysis (26). In contrast, glucose oxidation at high glucose, which reflects Krebs cycle velocity, was improved in GK islets by TE treatment. These results suggest that coupling between glycolysis and mitochondrial oxidation, which plays an important role in glucose-induced IS (33), is improved by TE treatment. Lactate production weakens coupling between glycolysis and mitochondrial oxidation by decreasing the pyruvate supply to mitochondria. In several studies, the overexpression of LDH-A in β-cells attenuated glucose-induced IS (34–36) with an increase in lactate production (34,37). In addition, lactate release from β-cells increases in parallel with a decrease in the glucose oxidation rate (36). These findings support the hypothesis that regulation of lactate production may play an important role in the improvement of metabolism-secretion coupling by TE treatment. In the current study, lactate production in GK islets was higher compared with that in control, as shown in a previous study (38), and it was reduced by TE treatment. The protein expression level of LDH-A, an enzyme that catalyzes the reaction from pyruvate and NADH to lactate and NAD^+, was 8.6-fold higher in GK islets compared with

TABLE 4
ATP production by mitochondria fraction from islets

Experimental conditions	Wistar rat		GK rat	
	C	TE	C	TE
0.5 mmol/L succinate	2.86 ± 0.42	2.58 ± 0.15	2.43 ± 0.27	2.18 ± 0.21
0.5 mmol/L succinate + 1 μmol/L antimycin A	0.40 ± 0.03	0.46 ± 0.02	0.36 ± 0.00	0.36 ± 0.00
1 mmol/L succinate + 1 μmol/L rotenone	3.96 ± 0.48	3.55 ± 0.26	2.92 ± 0.22	2.71 ± 0.48
1 mmol/L glutamate + 1 mmol/L malate	0.92 ± 0.23	0.86 ± 0.14	0.87 ± 0.13	0.90 ± 0.14
1 mmol/L pyruvate + 1 mmol/L malate	1.32 ± 0.38	1.17 ± 0.29	1.27 ± 0.22	1.23 ± 0.22
0.5 mmol/L TMPD + 2 mmol/L ascorbate	5.42 ± 0.41	4.91 ± 0.15	6.27 ± 0.62	5.94 ± 0.54
1 mmol/L G3P	0.92 ± 0.14	3.03 ± 0.17†	0.69 ± 0.05	1.50 ± 0.12†

Islets were cultured with or without TE for 12 h. Mitochondrial suspension was obtained from control (C) or TE-treated islets (TE). Mitochondrial ATP production is indicated as the ratio to ATP production from adenylate kinase to normalize the mass of the intact mitochondria obtained, which was determined from the same sample in parallel incubation. Data are given as the mean ± SE of three different experiments. †$P < 0.01$ vs. control without TE.

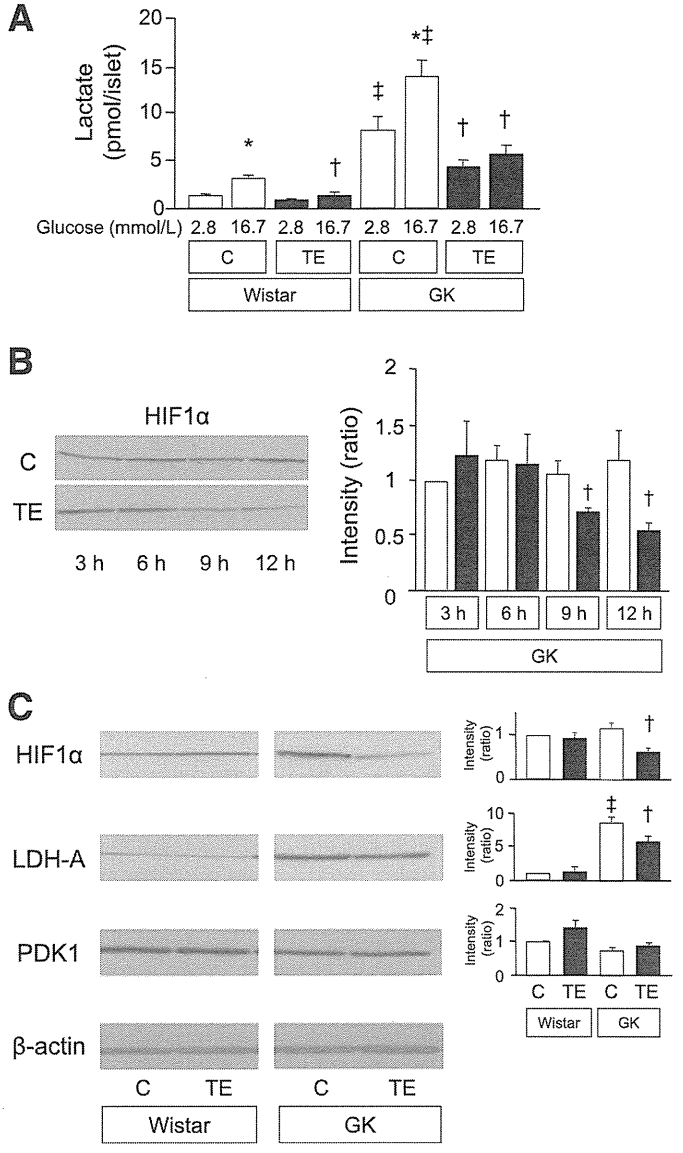

FIG. 4. Effects of TE treatment on lactate production and HIF1α signaling. Islets were cultured without (control [C]; open bars) or with TE (black bars) for 12 h. *A*: Effects of TE treatment on lactate production in Wistar and GK islets. After cultured islets were preincubated under 2.8 mmol/L glucose for 30 min, 20 islets were batch incubated in the medium containing 2.8 and 16.7 mmol/L glucose for 60 min at 37°C, and released lactate in the medium was measured. Values are means ± SE of 13 determinations from three (Wistar) and four (GK) experiments. *B*: Time course of HIF1α protein levels in GK and Wistar islets during TE treatment using whole-islet lysates. Islets were cultured without (C; open bars) or with TE (closed bars) for indicated hours. The bar graphs are expressed relative to 3 h–cultured control values corrected by β-actin level. The values are means ± SE of determinations from three different experiments. Representative blot panels are shown. *C*: Effect of TE treatment on protein levels of HIF1α and HIF1α downstream target proteins in whole lysate of Wistar and GK islets. Representative blot (*left*) and quantification data (*right*) are shown. The bar graphs are expressed relative to Wistar without TE treatment values corrected by β-actin level. The values are means ± SE of determinations from three different experiments. *P < 0.01 vs. corresponding 2.8 mmol/L glucose; †P < 0.01 vs. corresponding control without TE; ‡P < 0.01 vs. corresponding Wistar.

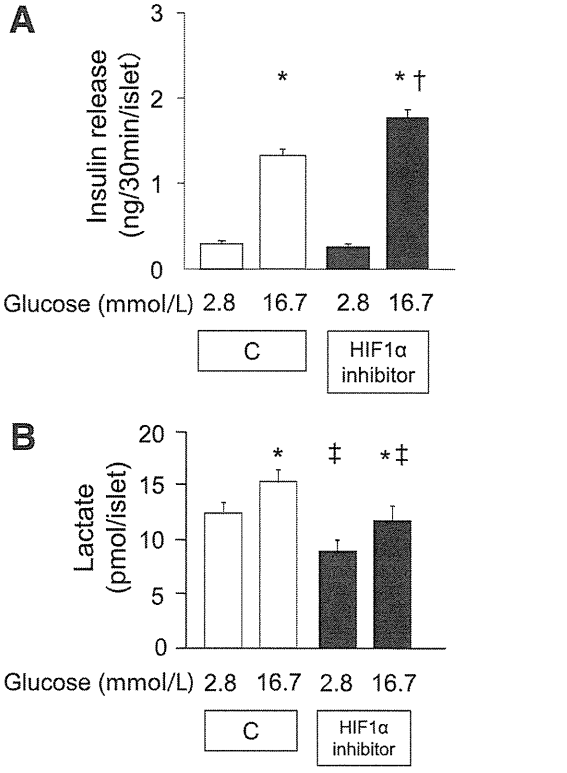

FIG. 5. Effects of HIF1α inhibitor on IS and lactate production in GK islets. Islets were cultured without (control [C]; open bars) or with 1 μmol/L HIF1α inhibitor (black bars) for 12 h. *A*: Insulin secretion. After cultured islets were preincubated with 2.8 mmol/L glucose for 30 min, IS during incubation for 30 min in the presence of 2.8 and 16.7 mmol/L glucose was measured in islets. Data are shown as means ± SE of 25 determinations from three experiments. *P < 0.01 vs. corresponding 2.8 mmol/L glucose; †P < 0.01 vs. 16.7 mmol/L glucose in control. *B*: Lactate production. After cultured islets were preincubated under 2.8 mmol/L glucose for 30 min, islets were batch incubated in the medium containing 2.8 and 16.7 mmol/L glucose for 60 min, and released lactate in the medium was measured. Values are means ± SE of 12 determinations from three experiments. *P < 0.01 vs. corresponding 2.8 mmol/L glucose; ‡P < 0.01 vs. corresponding control without HIF1α inhibitor.

control Wistar islets, and was reduced by ~30% after TE treatment. In nondiabetic pancreatic β-cells, low LDH activity together with high mGPDH activity may act as a device to transfer NADH in the cytosol to the mitochondria and reduce lactate production by decreasing the NADH level in cytosol (39). In GK islets, enhanced LDH activity and reduced mGPDH activity might produce lactate overproduction and reduce mitochondrial oxidation by decreasing the supply of pyruvate and reducing equivalents to mitochondria and by an increase in the availability of cytosolic NADH to produce lactate from pyruvate as well. In this case, reduced LDH activity and increased mGPDH activity by TE treatment may well have decreased lactate overproduction and ameliorated metabolism-secretion coupling in GK islets.

These metabolic profiles in GK islets resemble the Warburg effect, characteristic aerobic metabolism in cancer cells by which lactate is overproduced from glucose even under nonhypoxic conditions (40). HIF1α is a transcription factor that functions as a master regulator of oxygen homeostasis and upregulates the expression of *LDH* (41). HIF1α activity is controlled at the level of protein stability. When oxygen is present, two proline residues in the oxygen-dependent degradation domain of HIF1α are hydroxylated by the prolylhydroxylase enzymes (PHDs) (42). These hydroxylated motifs allow capture by the von Hippel-Lindau protein that forms the recognition component of an E3 ubiquitin ligase complex, which targets the hydroxylated HIF1α for polyubiquitination and proteasomal degradation (43). In the current study, TE treatment showed a time-dependent decrease in HIF1α protein levels

in GK islets and 50% reduction compared with that in nontreated GK islets at 12-h culture, which could reduce LDH-A protein in TE-treated GK islets. The Warburg effect is usually thought of as a high rate of glycolysis. Since TE treatment did not affect glucokinase activity, which determines glycolytic velocity in β-cells, alteration in the HIF1α level in the pathophysiological range may not affect glycolytic velocity in β-cells. In this respect, lactate overproduction in GK islets differs from the typical Warburg effect.

HIF1α downregulates the expression of GLUT2 and glucokinase and upregulates PDK-1, which inactivates pyruvate dehydrogenase and suppresses metabolism in the Krebs cycle (44) in islets of von Hippel-Lindau gene (*vhl*)-deficient mice (45). On the contrary, TE treatment did not affect the glucokinase activity and protein level of PDK-1 in GK islets. This discrepancy is not fully understood, but one possibility is that the expression level of HIF1α may be higher than the pathophysiological level in *vhl*-deficient islets. This is supported by the fact that glucose-induced IS is impaired severely and almost abolished in *vhl*-deficient islets. The transcript level of *LDH-A* in *vhl*-deficient islets is about 20-fold higher compared with control islets, which is much higher than that of *PDK-1* (~5-fold) (46). This suggests that the expression of LDH-A is more readily affected by HIF1α expression than that of PDK-1.

An increase in the basal HIF1α level in GK islets was not found compared with that in Wistar islets. In contrast, basal levels of LDH-A in GK islets was prominently increased compared with that in Wistar islets, suggesting that regulators other than HIF1α may play an important role in the enhancement of basal LDH-A in GK islets. However, our finding in the current study remains valid, as ROS-dependent regulation of LDH-A by HIF1α, which plays an important role in lactate overproduction and impaired glucose-induced IS in GK islets, was established. In addition, the involvement of HIF1α in lactate overproduction was shown clearly by the finding that HIF1α inhibitor treatment restored high glucose–induced IS and suppressed lactate production in GK islets. ROS inhibits PHD activity and stabilizes HIF1α (47,48). In GK islets, an excess amount of ROS may inhibit PHD activity and stabilize the HIF1α protein. Thus, TE treatment may recover PHD activity by reducing the ROS level and decreasing the HIF1α protein level to eventually ameliorate metabolism-secretion coupling in GK islets.

In conclusion, we show that 12-h suppression of endogenous ROS, including O_2^- and H_2O_2, improves impaired metabolism-secretion coupling in GK islets. Our results suggest that lactate overproduction plays an important role in impaired metabolism-secretion coupling in diabetic β-cells; ROS reduction improves mitochondrial metabolism by suppressing lactate overproduction through the inhibition of HIF1α stabilization.

ACKNOWLEDGMENTS

This study was supported by a Research Grant on Nanotechnical Medicine from the Ministry of Health, Labour and Welfare of Japan; scientific research grants; a grant from the Innovation Cluster Kansai project of the Ministry of Education, Culture, Sports, Science and Technology of Japan; and a grant from CREST of the Japan Science and Technology Cooperation.

No potential conflicts of interest relevant to this article were reported.

M.S. researched data, contributed to the discussion, wrote the manuscript, and reviewed and edited the manuscript. S.F. contributed to the discussion, wrote the manuscript, and reviewed and edited the manuscript. Y.S., Y.N., E.M., G.Y., H.S., Y.T., and K.O. researched data. K.N. and N.I. contributed to the discussion, and reviewed and edited the manuscript. S.F. is the guarantor of this work and, as such, had full access to all the data in the study and takes responsibility for the integrity of the data and the accuracy of the data analysis.

Parts of this study were presented in abstract form at the 72nd Scientific Sessions of the American Diabetes Association, Philadelphia, Pennsylvania, 8–12 June 2012.

The authors thank C. Kotake and M. Akazawa (Kyoto University) for technical assistance.

REFERENCES

1. Fujimoto S, Mukai E, Inagaki N. Role of endogenous ROS production in impaired metabolism-secretion coupling of diabetic pancreatic β cells. Prog Biophys Mol Biol 2011;107:304–310
2. Fujimoto S, Nabe K, Takehiro M, et al. Impaired metabolism-secretion coupling in pancreatic β-cells: role of determinants of mitochondrial ATP production. Diabetes Res Clin Pract 2007;77(Suppl 1):S2–S10
3. Bindokas VP, Kuznetsov A, Sreenan S, Polonsky KS, Roe MW, Philipson LH. Visualizing superoxide production in normal and diabetic rat islets of Langerhans. J Biol Chem 2003;278:9796–9801
4. Turrens JF. Mitochondrial formation of reactive oxygen species. J Physiol 2003;552:335–344
5. Guichard C, Moreau R, Pessayre D, Epperson TK, Krause KH. NOX family NADPH oxidases in liver and in pancreatic islets: a role in the metabolic syndrome and diabetes? Biochem Soc Trans 2008;36:920–929
6. Grankvist K, Marklund SL, Täljedal IB. CuZn-superoxide dismutase, Mn-superoxide dismutase, catalase and glutathione peroxidase in pancreatic islets and other tissues in the mouse. Biochem J 1981;199:393–398
7. Tiedge M, Lortz S, Munday R, Lenzen S. Complementary action of antioxidant enzymes in the protection of bioengineered insulin-producing RINm5F cells against the toxicity of reactive oxygen species. Diabetes 1998;47:1578–1585
8. Maechler P, Jornot L, Wollheim CB. Hydrogen peroxide alters mitochondrial activation and insulin secretion in pancreatic beta cells. J Biol Chem 1999;274:27905–27913
9. Kominato R, Fujimoto S, Mukai E, et al. Src activation generates reactive oxygen species and impairs metabolism-secretion coupling in diabetic Goto-Kakizaki and ouabain-treated rat pancreatic islets. Diabetologia 2008; 51:1226–1235
10. Mukai E, Fujimoto S, Sato H, et al. Exendin-4 suppresses SRC activation and reactive oxygen species production in diabetic Goto-Kakizaki rat islets in an Epac-dependent manner. Diabetes 2011;60:218–226
11. Kajikawa M, Fujimoto S, Tsuura Y, et al. Ouabain suppresses glucose-induced mitochondrial ATP production and insulin release by generating reactive oxygen species in pancreatic islets. Diabetes 2002;51:2522–2529
12. Nassar T, Kadery B, Lotan C, Da'as N, Kleinman Y, Haj-Yehia A. Effects of the superoxide dismutase-mimetic compound tempol on endothelial dysfunction in streptozotocin-induced diabetic rats. Eur J Pharmacol 2002; 436:111–118
13. Dawson DA, Masayasu H, Graham DI, Macrae IM. The neuroprotective efficacy of ebselen (a glutathione peroxidase mimic) on brain damage induced by transient focal cerebral ischaemia in the rat. Neurosci Lett 1995;185:65–69
14. Tang C, Han P, Oprescu AI, et al. Evidence for a role of superoxide generation in glucose-induced β-cell dysfunction in vivo. Diabetes 2007;56: 2722–2731
15. Wang XD, Vatamaniuk MZ, Wang SK, Roneker CA, Simmons RA, Lei XG. Molecular mechanisms for hyperinsulinaemia induced by overproduction of selenium-dependent glutathione peroxidase-1 in mice. Diabetologia 2008;51:1515–1524
16. Fujimoto S, Ishida H, Kato S, et al. The novel insulinotropic mechanism of pimobendan: direct enhancement of the exocytotic process of insulin secretory granules by increased Ca^{2+} sensitivity in β-cells. Endocrinology 1998;139:1133–1140
17. Oliveira HR, Verlengia R, Carvalho CR, Britto LR, Curi R, Carpinelli AR. Pancreatic β-cells express phagocyte-like NAD(P)H oxidase. Diabetes 2003;52:1457–1463

18. Takasu N, Yamada T, Shimizu Y. Generation of H_2O_2 is regulated by cytoplasmic free calcium in cultured porcine thyroid cells. Biochem Biophys Res Commun 1987;148:1527–1532
19. Nabe K, Fujimoto S, Shimodahira M, et al. Diphenylhydantoin suppresses glucose-induced insulin release by decreasing cytoplasmic H^+ concentration in pancreatic islets. Endocrinology 2006;147:2717–2727
20. Shimodahira M, Fujimoto S, Mukai E, et al. Rapamycin impairs metabolism-secretion coupling in rat pancreatic islets by suppressing carbohydrate metabolism. J Endocrinol 2010;204:37–46
21. Takehiro M, Fujimoto S, Shimodahira M, et al. Chronic exposure to β-hydroxybutyrate inhibits glucose-induced insulin release from pancreatic islets by decreasing NADH contents. Am J Physiol Endocrinol Metab 2005;288:E372–E380
22. Radu RG, Fujimoto S, Mukai E, et al. Tacrolimus suppresses glucose-induced insulin release from pancreatic islets by reducing glucokinase activity. Am J Physiol Endocrinol Metab 2005;288:E365–E371
23. Gardner RS. A sensitive colorimetric assay for mitochondrial alpha-glycerophosphate dehydrogenase. Anal Biochem 1974;59:272–276
24. MacDonald MJ. High content of mitochondrial glycerol-3-phosphate dehydrogenase in pancreatic islets and its inhibition by diazoxide. J Biol Chem 1981;256:8287–8290
25. Miwa I, Fukatsu H, Toyoda Y, Okuda J. Anomeric preference of glucose utilization in human erythrocytes loaded with glucokinase. Biochem Biophys Res Commun 1990;173:201–207
26. Meglasson MD, Matschinsky FM. Pancreatic islet glucose metabolism and regulation of insulin secretion. Diabetes Metab Rev 1986;2:163–214
27. Choi JH, Cho HK, Choi YH, Cheong J. Activating transcription factor 2 increases transactivation and protein stability of hypoxia-inducible factor 1α in hepatocytes. Biochem J 2009;424:285–296
28. Mysore TB, Shinkel TA, Collins J, et al. Overexpression of glutathione peroxidase with two isoforms of superoxide dismutase protects mouse islets from oxidative injury and improves islet graft function. Diabetes 2005;54:2109–2116
29. Lortz S, Tiedge M. Sequential inactivation of reactive oxygen species by combined overexpression of SOD isoforms and catalase in insulin-producing cells. Free Radic Biol Med 2003;34:683–688
30. Zhang CY, Baffy G, Perret P, et al. Uncoupling protein-2 negatively regulates insulin secretion and is a major link between obesity, β cell dysfunction, and type 2 diabetes. Cell 2001;105:745–755
31. Yoshihara E, Fujimoto S, Inagaki N, et al. Disruption of TBP-2 ameliorates insulin sensitivity and secretion without affecting obesity. Nat Commun 2010;1:127
32. Östenson CG, Abdel-Halim SM, Rasschaert J, et al. Deficient activity of FAD-linked glycerophosphate dehydrogenase in islets of GK rats. Diabetologia 1993;36:722–726
33. Malmgren S, Nicholls DG, Taneera J, et al. Tight coupling between glucose and mitochondrial metabolism in clonal β-cells is required for robust insulin secretion. J Biol Chem 2009;284:32395–32404
34. Zhao C, Rutter GA. Overexpression of lactate dehydrogenase A attenuates glucose-induced insulin secretion in stable MIN-6 β-cell lines. FEBS Lett 1998;430:213–216
35. Ainscow EK, Zhao C, Rutter GA. Acute overexpression of lactate dehydrogenase-A perturbs beta-cell mitochondrial metabolism and insulin secretion. Diabetes 2000;49:1149–1155
36. Alcazar O, Tiedge M, Lenzen S. Importance of lactate dehydrogenase for the regulation of glycolytic flux and insulin secretion in insulin-producing cells. Biochem J 2000;352:373–380
37. MacDonald MJ. Estimates of glycolysis, pyruvate (de)carboxylation, pentose phosphate pathway, and methyl succinate metabolism in incapacitated pancreatic islets. Arch Biochem Biophys 1993;305:205–214
38. Ling ZC, Efendic S, Wibom R, et al. Glucose metabolism in Goto-Kakizaki rat islets. Endocrinology 1998;139:2670–2675
39. Sekine N, Cirulli V, Regazzi R, et al. Low lactate dehydrogenase and high mitochondrial glycerol phosphate dehydrogenase in pancreatic β-cells. Potential role in nutrient sensing. J Biol Chem 1994;269:4895–4902
40. Koppenol WH, Bounds PL, Dang CV. Otto Warburg's contributions to current concepts of cancer metabolism. Nat Rev Cancer 2011;11:325–337
41. Gordan JD, Thompson CB, Simon MC. HIF and c-Myc: sibling rivals for control of cancer cell metabolism and proliferation. Cancer Cell 2007;12:108–113
42. Jaakkola P, Mole DR, Tian YM, et al. Targeting of HIF-α to the von Hippel-Lindau ubiquitylation complex by O_2-regulated prolyl hydroxylation. Science 2001;292:468–472
43. Maxwell PH, Wiesener MS, Chang GW, et al. The tumour suppressor protein VHL targets hypoxia-inducible factors for oxygen-dependent proteolysis. Nature 1999;399:271–275
44. Kim JW, Tchernyshyov I, Semenza GL, Dang CV. HIF-1-mediated expression of pyruvate dehydrogenase kinase: a metabolic switch required for cellular adaptation to hypoxia. Cell Metab 2006;3:177–185
45. Cantley J, Selman C, Shukla D, et al. Deletion of the von Hippel-Lindau gene in pancreatic β cells impairs glucose homeostasis in mice. J Clin Invest 2009;119:125–135
46. Puri S, Cano DA, Hebrok M. A role for von Hippel-Lindau protein in pancreatic β-cell function. Diabetes 2009;58:433–441
47. Gerald D, Berra E, Frapart YM, et al. JunD reduces tumor angiogenesis by protecting cells from oxidative stress. Cell 2004;118:781–794
48. Kaelin WG Jr, Ratcliffe PJ. Oxygen sensing by metazoans: the central role of the HIF hydroxylase pathway. Mol Cell 2008;30:393–402

Molecular Genetics and Metabolism 109 (2013) 112–117

Contents lists available at SciVerse ScienceDirect

Molecular Genetics and Metabolism

journal homepage: www.elsevier.com/locate/ymgme

Exome sequencing identifies a new candidate mutation for susceptibility to diabetes in a family with highly aggregated type 2 diabetes

Daisuke Tanaka [a], Kazuaki Nagashima [a], Mayumi Sasaki [a], Shogo Funakoshi [a], Yasushi Kondo [a], Koichiro Yasuda [b], Akio Koizumi [c], Nobuya Inagaki [a,*]

[a] Department of Diabetes and Clinical Nutrition, Graduate School of Medicine, Kyoto University, 54 Shogoin-Kawahara-cho, Sakyo-ku, Kyoto, 606-8507, Japan
[b] Saiseikai Noe Hospital, 1-3-25 Furuichi, Joto-ku, Osaka, 536-0001, Japan
[c] Department of Health and Environmental Sciences, Graduate School of Medicine, Kyoto University, Yoshidakonoe-cho, Sakyo-ku, Kyoto, 606-8501, Japan

ARTICLE INFO

Article history:
Received 15 January 2013
Received in revised form 13 February 2013
Accepted 13 February 2013
Available online 21 February 2013

Keywords:
Genetics of type 2 diabetes
Linkage analysis
Exome sequencing
EEA1

ABSTRACT

The aim of this study was to investigate the genetic background of familial clustering of diabetes using genome-wide linkage analysis combined with exome sequencing. We recruited a Japanese family with a 3-generation history of diabetes. The family comprised 16 members, 13 having been diagnosed with diabetes. Nine members had been diagnosed before the age of 40. Linkage analysis was performed assuming an autosomal dominant model. Linkage regions were observed on chromosomes 4q34, 5q11–q13, and 12p11–q22 and the logarithm of odds (LOD) scores were 1.80. To identify the susceptibility variants, we performed exome sequencing of an affected family member. We predicted that the familial clustering of diabetes is caused by a rare non-synonymous variant, and focused our analysis on non-synonymous variants absent in dbSNP131. Exome sequencing identified 10 such variants in the linkage regions, 7 of which were concordant with the affection status in the family. One hundred five normal subjects and 67 lean diabetes subjects were genotyped for the 7 variants; the only variant found to be significantly more frequent in the diabetes subjects than in the normal subjects was the N1072K variant of the early endosome antigen 1 (EEA1) gene (0 in normal subjects and 4 in diabetes subjects, $p=0.022$). We therefore propose that the N1072K variant of the EEA1 gene is a candidate mutation for susceptibility to diabetes in the Japanese population.

1. Introduction

In Japan, 11.2% of all adults suffer from diabetes mellitus, and its increasing prevalence is a serious concern [1]. Most of these patients have type 2 diabetes. While recent advances in genome-wide association studies (GWAS) have revealed over 60 type 2 diabetes susceptibility loci, all of them account for less than 20% of the genetic background of the disease [2–4]. GWAS is based on the common disease-common variant hypothesis, and rare disease variants with large effect size are frequently missed [5]. Approaches other than GWAS are necessary to elucidate the greater part of the genetic background of type 2 diabetes.

A family-based study is a promising approach to identify rare disease variants with large effect size [6]. Familial clustering of diabetes is frequently observed and the typical example of familial diabetes caused by rare disease variants is Maturity Onset Diabetes of the Young (MODY). However, in most families in Japan, familial clustering cannot be attributed to mutations of the known 6 MODY genes (*HNF4A*, *GCK*, *HNF1A*, *PDX1*, *HNF1B*, and *NEUROD1*) despite intensive linkage analyses and candidate-gene screening [7,8], and the genetic predisposition in such families has not been ascertained.

Recently, exome sequencing has become a powerful strategy for identifying causative genes for a number of Mendelian disorders [9]. As exome sequencing identifies thousands of exonic variants, a selection strategy to identify the particular variant causing the disorder is necessary.

In the present study, we combined linkage analysis and exome sequencing to identify the causal genetic variant in a family with highly aggregated diabetes and elucidated the genetic background of type 2 diabetes in Japan.

2. Material and methods

2.1. Family members

We recruited a Japanese family with a 3-generation family history of diabetes mellitus (Fig. 1). Medical history was gained from the family members and body mass index (BMI) and HbA_{1c} levels were measured in the year 2010 at entry to the study. All study participants

Abbreviations: LOD, Logarithm of Odds; EEA1, Early Endosome Antigen 1; GWAS, Genome-Wide Association Study; MODY, Maturity Onset Diabetes of the Young; HNF4A, Hepatocyte Nuclear Factor 4 Alpha; BMI, Body Mass Index; SNP, Single Nucleotide Polymorphism; CNV, Copy Number Variation; MAF, Minor Allele Frequency.

* Corresponding author. Fax: +81 75 771 6601.
E-mail address: inagaki@metab.kuhp.kyoto-u.ac.jp (N. Inagaki).

1096-7192/$ – see front matter © 2013 Elsevier Inc. All rights reserved.
http://dx.doi.org/10.1016/j.ymgme.2013.02.010

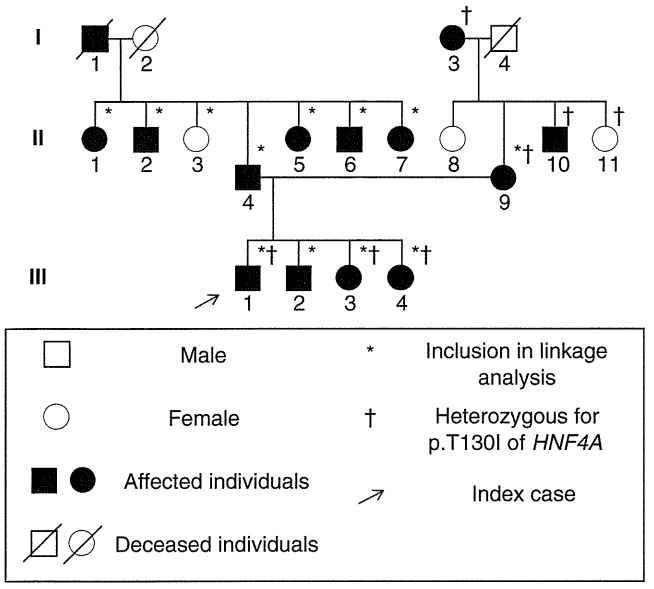

Fig. 1. A pedigree with familial aggregated diabetes mellitus.

from the family were negative for glutamic acid decarboxylase antibody. Affected status of the participants was determined in two ways. First, if participants had been diagnosed with diabetes and treated with oral antidiabetic drugs or insulin injection, they were regarded as affected. Second, if participants had not been treated with oral antidiabetic drugs or insulin injection, they underwent HbA_{1c} measurement. If their HbA_{1c} levels were $\geq$6.5% [10], they were also regarded as affected. The clinical features of family members are shown in Table 1.

Deceased individual I-1 had diabetes according to the interview with family members. There was no information suggesting consanguineous marriage in the family. Some of the individuals in generation II had offspring and none of them except III-1, 2, 3, and 4, had diabetes according to the information from family members.

2.2. Normoglycemic controls and diabetes subjects

We selected normoglycemic controls from the participants in an annual medical check-up program performed in Japan. Nine-hundred ninety local residents (430 men, 560 women) were recruited in the program and consented to donate their DNA. From 2002 to 2007, participants underwent physical examination and blood tests including fasting plasma glucose and HbA_{1c} every year. Subjects defined as normoglycemic controls had the following characteristics: both HbA_{1c} and fasting plasma glucose below the screening standards for the diagnosis of diabetes (HbA_{1c}<6.0% and fasting plasma glucose<5.5 mmol/l [10]) during 5-year follow-up span, and age$\geq$55. The number of subjects that satisfied the definition was 206 (81 men, 125 women). For genotyping, 105 normoglycemic controls were randomly selected (Supplementary Table 1), because genotyping of 210 normal chromosomes is necessary to achieve 80% power to detect a polymorphism present in 1% of the population [11]. We recruited lean diabetes subjects from participants in another medical check-up program performed in Japan. One hundred and thirty-eight participants had been diagnosed with diabetes and 68 were lean (BMI<25). DNA was available from 67 of the lean diabetes subjects (Supplementary Table 1). Another, unrelated 64 diabetes subjects with family history had visited collaborating hospitals in Japan and donated their DNA. Genomic DNA was extracted from blood samples with a QIAamp DNA Blood Mini kit (Qiagen).

Table 1
Characteristics of the family members.

ID	Age	Sex	BMI	HbA_{1c} (%)	Age when diagnosed	Current therapy
I-3	88	F	16.8	5.6	N/A	Oral drug
II-1	78	F	23.8	6.8	35	Oral drug
II-2	75	M	22.7	7.5	35	Oral drug
II-3	72	F	28.2	6.0		
II-4	68	M	23.3	9.2	35	Oral drug
II-5	65	F	24.6	6.8	65	Diet
II-6	62	M	22.4	8.1	30	Diet
II-7	60	F	23.3	7.6	35	Insulin 10 U/d
II-8	68	F	26.7	5.7		
II-9	66	F	23.9	7.8	44	Oral drug
II-10	63	M	20.5	7.4	N/A	Oral drug
II-11	61	F	21.2	5.4		
III-1	40	M	26.0	8.5	30	Oral drug
III-2	39	M	29.0	7.6	38	Oral drug
III-3	36	F	29.9	6.6	36	Diet
III-4	26	F	29.1	6.6	26	Diet

2.3. Linkage analysis

We performed a genome-wide linkage analysis using GENEHUNTER (version 2.1) software [12] with ABI Prism Linkage Mapping Set Version 2.5 (382 markers for 22 autosomes; Applied Biosystems) and other microsatellite fine markers designed according to information from the UniSTS map (http://www.ncbi.nlm.nih.gov/genome/sts/). A multipoint parametric linkage analyses for autosomes were performed assuming an autosomal dominant model because the 3-generation family history is suggestive of autosomal dominant mode of inheritance [6]. Since sensitivity analyses for the disease allele frequency by changing it from 0.01 to 0.00001 suggested negligible effects on LOD score, the disease allele frequency was set at 0.00001 and a phenocopy frequency of 0.00001 was assumed. Affected family members with known diabetes susceptibility variants were considered as having unknown phenotype. The purpose of including members assigned as unknown was to increase the accuracy of haplotype estimation in members assigned as affected, although inclusion did not increase the statistical power. Population allele frequencies for each microsatellite marker were assigned equal portions for individual alleles. We used a 2-stage design: first, all chromosomal regions were screened by genotyping at an approximately 10 cM density (screening), and the regions where LOD scores were highest were considered potentially interesting. Second, these regions were further finely mapped at approximately 1- to 2-cM densities (fine mapping). Haplotypes were constructed with GENEHUNTER.

2.4. Sanger sequencing

We directly sequenced the coding exons of 6 MODY genes (*HNF4A*, *GCK*, *HNF1A*, *PDX1*, *HNF1B*, and *NEUROD1*) by Sanger method. Forward and reverse PCR primers for each exon were selected in an intronic sequence 50 bp away from the intron/exon boundaries. PCR products were run on 2% agarose gel, and the appropriate bands were excised and then purified with the use of the QIAquick Gel Extraction Kit (Qiagen). Sequencing results were analyzed on an ABI 3130 genetic analyzer (Applied Biosystems). Sanger sequencing was also used to confirm the single nucleotide polymorphisms (SNPs) identified in exome sequencing. Sequencing primer data will be provided on request.

2.5. Copy number variation (CNV) analysis

We selected CNVs that overlapped with MODY genes (*HNF1A*, *HNF1B*, and *GCK*, Supplementary Table 2). We performed real-time PCR to determine CNV status on normal control and family members. TaqMan probes designed by the manufacturer (Applied Biosystems, Supplementary Table 2), were used to target the specific regions. *RNase P* (Taqman Copy Number Reference Assay, Applied Biosystems)